



GCM mapping Gedved

Report number 23-06-2017, June 2017





1. INDHOLDSFORTEGNELSE

1. Indholdsfortegnelse	1
2. Project information	2
3. DUALEM-421s	3
3.1 Setup and functionality	3
3.2 Sensitivity distribution	4
3.3 Disadvantages.....	6
3.4 The resistivity of various soil types	7
4. Data collection	9
4.1 Data drift quality control.....	9
5. Processing	12
6. Inversion	14
6.1 The SCI-method.....	14
6.2 Depth of Investigation.....	16
6.3 Mean-resistivity maps	17
7. Results	19
7.1 Quality control maps	20
Model Location and GCM Lines	20
Data Residual.....	20
Number of data points.....	20
Depth of Investigation (DOI).....	20
7.2 Raw resistivity data maps.....	21
7.3 Magnetic susceptibility.....	22
7.4 Mean Resistivity	23
7.5 Profiles	24



2. PROJECT INFORMATION

GCM mapping – Gedved	
Contact person	Jesper Pedersen, Aarhus University Helle Blæsbjerg, Central Denmark Region Rolf Johnsen, Central Denmark Region Jes Pedersen, Central Denmark Region Keld Rasmussen, Horsens Municipality Rasmus Rønde Møller, Horsens Municipality Martin Mogensen, Go-Gris
Locality	Gedved, Denmark
Field period	5 th – 7 th of September, 2017
Line spacing	Line spacing (10-15 meter)
Total number of measurements	117.179 measurements (equivalent to 117 km)
Report	Prepared by: Jesper Pedersen, Aarhus University Anders V. Christiansen, Aarhus University Esben Auken, Aarhus University Gianluca Fiandaca, Aarhus University Simon Ejlertsen, Aarhus University Søren Møller Dath, Aarhus University

Table 1. Project information



3. DUALEM-421S

3.1 Setup and functionality

The DUALEM-421S is a Ground Conductivity Meter (GCM) instrument using electromagnetic induction to estimate the electrical resistivity distribution in the subsurface.

The instrument consists of a horizontal transmitter coil mounted at one end of a 4-m long tube. Within the tube, three pairs of receiver coils are mounted at a distance of respectively 1, 2, and 4 m from the transmitter coil. In each pair of receiver coils one coil is placed horizontally (HCP-configuration) and the other vertically (PRP-configuration). See figure 1 and 2 for a sketch of the DUALEM-421S instrument. The DUALEM-421S instrument is pulled behind an ATV at a distance of approximately 4 m where it will not influence the measurements (see Figure 3).



Figure 1. Sketch of the transmitter (Tx) and receiver (Rx) coils in a DUALEM-421S system. For the HCP-configuration the Rx-coil is placed on the same horizontal plane as the transmitter coil. For the PRP-configuration the Rx-coil is perpendicular to the Tx-coil and centered around the Tx-coil's horizontal plane.



Figure 2. Sketch of the DUALEM-421S instrument. The transmitter coil (Tx) is placed at one end of the tube and the 3 receiver coil pairs (Rx) at a distance of 1, 2, and 4 m from the transmitter coil.

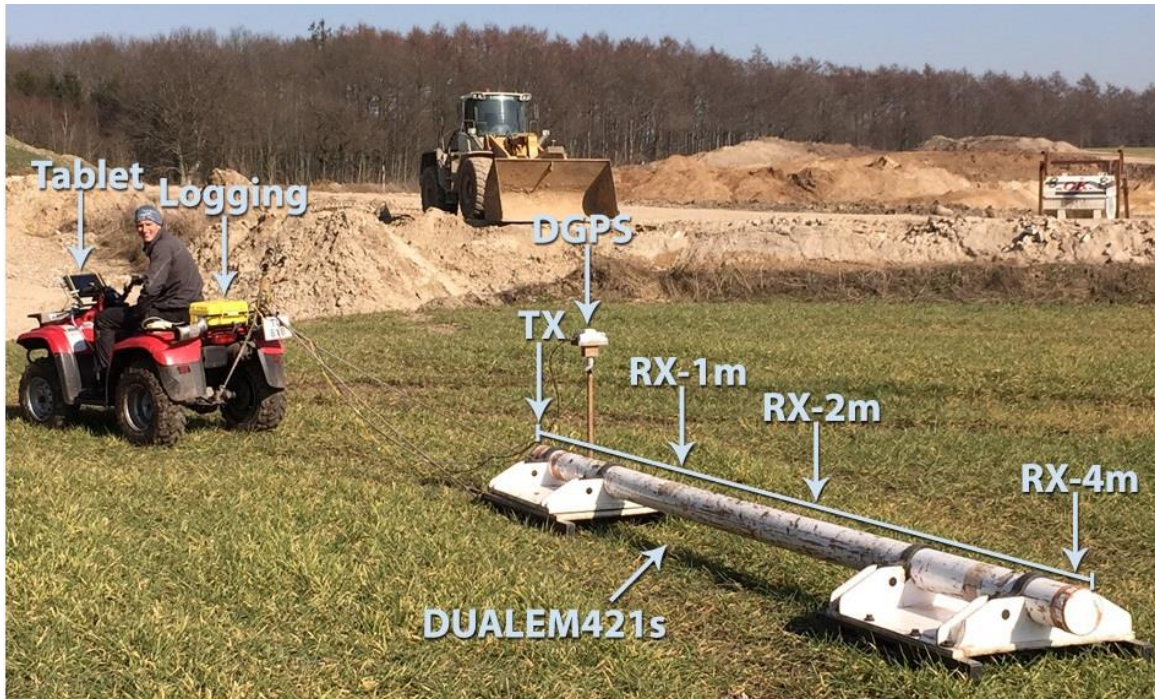


Figure 3. Field setup. The DUALEM-421s instrument is pulled by an ATV. The instrument is equipped with a GPS for accurate positioning of the measurements.

An alternating current is sent through the transmitter coil, forming a primary magnetic field in the ground, alternating at the same frequency as the current.

The alternations in the magnetic field induce an alternating electrical field in the ground, which again forms a alternating secondary magnetic field that can be measured by the receiver coils. This secondary magnetic field contains information about the ground's electrical properties.

The DUALEM-421s is a frequency domain system that continuously transmits a primary field with a frequency of 9 kHz. The receiver coils measure the secondary field's amplitude and phase. Amplitude and phase are measured in relation to the primary field.

3.2 Sensitivity distribution

The sensitivity of the subsurface layers at various depths depends on the resistivity of the layers (the geology), the choice of frequency, the distance between the transmitter and the receiver coils, and the orientation of the coils in relation to each other. For the DUALEM-421s-system the frequency and the geometry of the coils are



fixed, but since there are three pairs of receiver coils, a total of 6 independent configurations is achieved. For each of these 6 configurations both amplitude and phase are measured, but the phase is traditionally difficult to calibrate on these instruments and we have chosen not to use it in the interpretation. Thus, we get 6 data points per measurement. These 6 data points contain information about different parts of the ground, since they have different vertical sensitivity distributions. Generally, the HCP-configurations penetrate deeper than the PRP-configurations, and configurations with a longer coil distance penetrate deeper than configurations with a shorter coil distance.

For a HCP-configuration the 1D sensitivity function is described as:

$$S^{HCP}(z) = \frac{4z}{(1 + 4z^2)^{\frac{3}{2}}}$$

For PRP the 1D sensitivity function is expressed by:

$$S^{PRP}(z) = \frac{2}{(1 + 4z^2)^{\frac{3}{2}}}$$

For both equations z is a normalized depth, $z = d/r$, where d is depth and r is the distance between transmitter and receiver coils. The sensitivity functions for the 6 configurations are shown in Figure 4, where the left plot shows the above equations (normalized with the total sensitivity) and the right plot shows the cumulated sensitivities.

From the sensitivity functions, it can be seen that the PRP-configurations contain the most information at the surface whereas the HCP configurations have little sensitivity at the top with a distinct maximum somewhere below the surface.

In the summated sensitivity functions in Figure 4 an estimate of the focus depth is shown with a circle. The focus depth is indicated at the depth at which 50% of the sensitivity is reached. For the HCP configuration of 1 m the focus depth is ca. 0.87 m (1.73 m for a 2-m coil distance and 3.5 m for a 4-m coil distance). For the PRP configuration with a coil distance of 1.1 m the focus depth is found at ca. 0.32 m and correspondingly at 0.61 m with a coil distance of



2.1 m, and at 1.2 m for a PRP-configuration with a coil distance of 4.1 m. Hence, the HCP configurations have a deeper sensitivity-distribution than the PRP-configurations.

These indicated maximum sensitivities and focus depths are based on the assumption that the equipment measures from the ground surface. As this GCM equipment measures from 30 cm over the ground surface the values will be slightly less as some of the sensitivity is lost in the air.

The GCM-system is mounted on a sled, which is pulled by an ATV, thus achieving a fast and navigable system that can map many km per day.

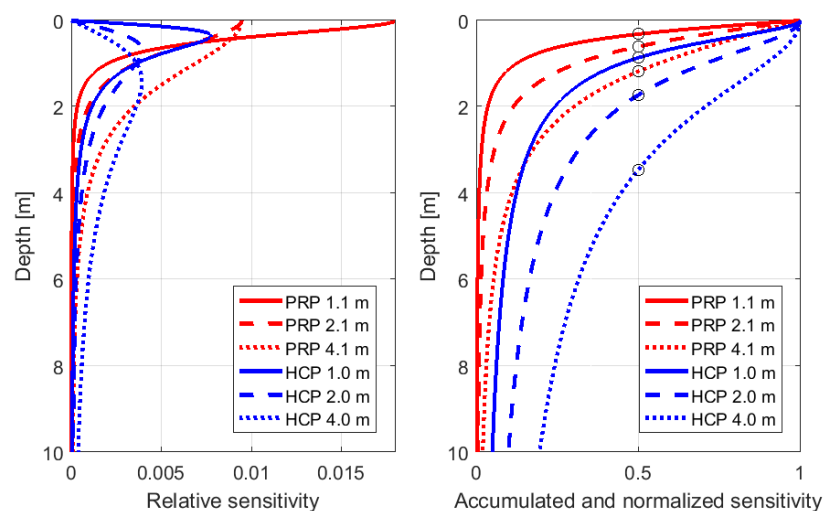


Figure 4. **Left:** Sensitivity function for HCP (blue curves), og PRP (red curves). **Right:** The integrated sensitivity function for HCP (blue curves) and PRP (red curves).

3.3 Disadvantages

Like all other electromagnetic methods, the GCM method is influenced by external sources of noise like fences, metal pipes in the ground, power lines etc. and it is necessary to measure somewhat away from these sources for them not to influence the measurements. The larger the source of noise the further away you need to be.

The DUALEM-421S instrument has 6 receiver coils and thus 6 data points are achieved for each measurement. Ideally, with 6 data points you can interpret 6 parameters – for instance the resistivity of 6 layers with fixed layer boundaries. In practice, more than 6



layers are used in the interpretation, and the layers are connected by lateral and vertical constraints in order to have a robust solution which at the same time complies with the expected geological variations. The relatively few data points and expected penetration depths must be taken into account when evaluating the results of the inversion.

3.4 The resistivity of various soil types

With the GCM method the resistivity in the ground can be measured to a depth of approximately 7 m. The measured resistivity depends on several factors like lithology, water content and the ion content in the water. Figure 5 shows the relative resistivity of different Danish lithologies in and the relation to water quality. Figure 6 shows the values of typical resistivities of Danish lithologies. Due to the chemical composition clay deposits are characterized by having a low resistivity while layers of sand or gravel have a high resistivity

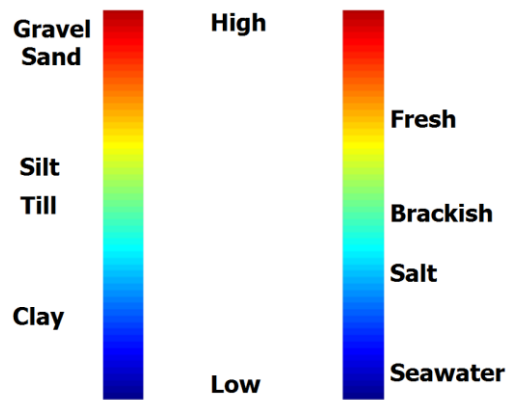


Figure 5. Relative resistivity of various lithologies and the relation to water quality.

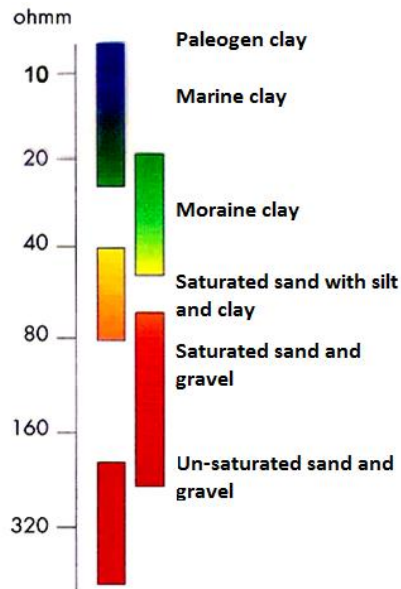


Figure 6. The resistivity of different Danish lithologies.



4. DATA COLLECTION

The data collection was carried out the 5th – 7th of September, 2016. The survey area was mapped with a 10-15 m line spacing and 117.179 measurements were collected during the mapping campaign (see *Figure 7*).

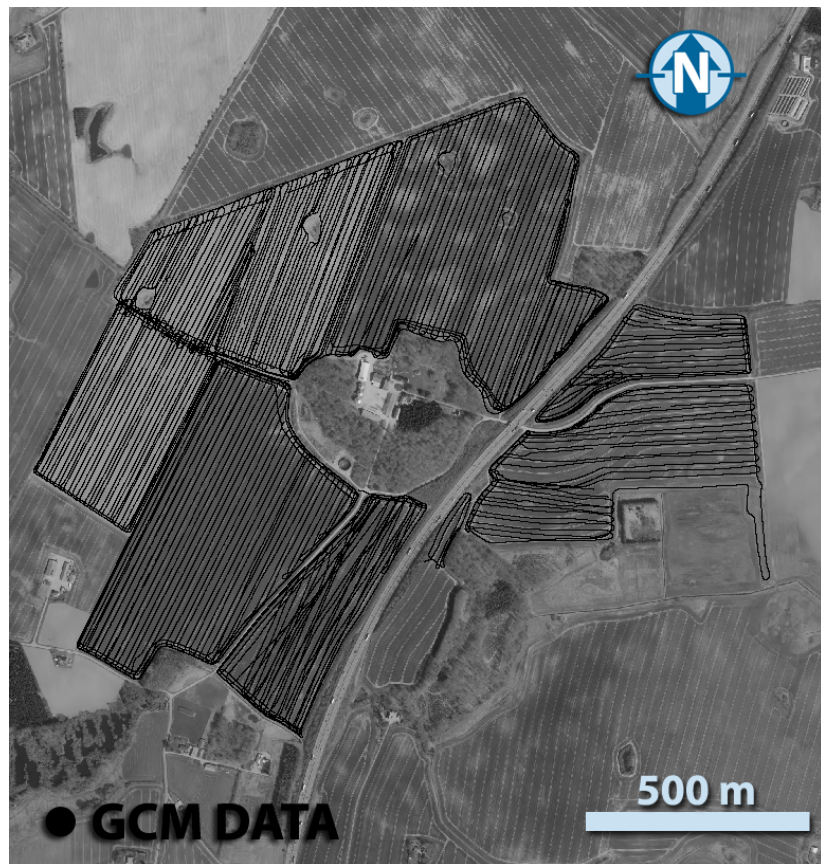


Figure 7. Map of measurements. Measurements are shown with black points.

4.1 Data drift quality control

With the DUALEM421 system the geometry, i.e. the distances between the transmitter coils and receiver coils, are presumed constant when interpreting the measured data. Potentially, changes in the presumed system geometry can result in faulty interpretations, since the calculated resistivity in the subsurface can be either too high or too low. This is called data drift. Changes in the system geometry are rarely seen, but can take place in case of for instance significant temperature changes in the instrument. High temperatures may make the receiver coils expand, which causes data drift, as the presumed system geometry is changed.



Another cause for data drift can be mapping in a rough terrain. If the instrument is handled roughly by bumping through rough terrain it can influence the internal placing of the transmitter and receiver coils.

In order to verify that data are not influenced by data drift a quality control point and/or line are established for each mapping area. The quality control point and line are GPS referenced. The point and line are measured twice with the GCM instrument, once before and once after the data collection on a daily basis during the survey period. The results of the measurements should be close to identical for all 6 receiver coil configurations. Should this not be the case a data shift can be applied to the affected data channels. The data for the Gedved survey was not affected by data drift as is seen in figure 8 which shows the repeated measurements for all six receiver coils from day 1 to 3 of the mapping. The small variations are well within acceptable limits.

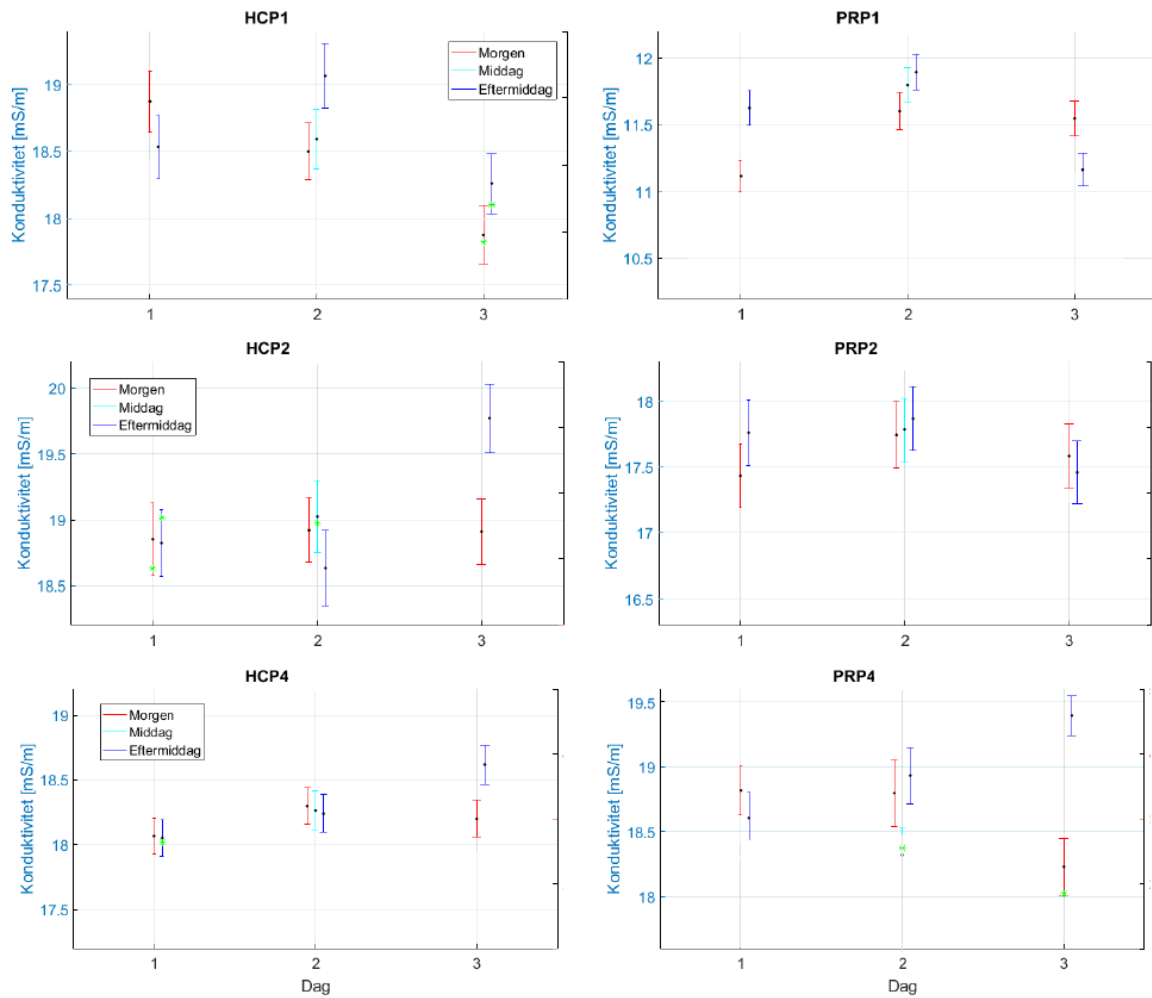


Figure 8. Results of the measurements from the control point for all six receiver coils. The control point was measured at least twice per day. Little or no variations were observed for the repeated measurements.



5. PROCESSING

The processing of the GCM data is carried out in the Aarhus Workbench. The objective of the processing is to make the data ready for inversion and interpretation. Only the amplitude data, not the phase, from the measurements are used. Generally, the data quality is good and only negative and noise influenced data have been removed in the processing. Negative and noise influenced data are mainly seen at the end of a line where instruments has been turned to start the next line. Further, the data have been averaged with a running mean filter. We achieve a raw measurement approximately every 30 cm, which after the filtering results in a measurement for every 1 m.

The uncertainty of the data has been estimated. This is done to assign more uncertainty to data measured on higher resistivities where the signal level is the lower. Typically, the noise from a GCM instrument is additive to the measured response, which is usually indicated in ppm (parts per million). From the instrument software, the measurements are indicated as apparent resistivity (ρ_a):

$$\sigma_a = \frac{1}{\rho_a} = \frac{4}{\omega \mu_0 s^2} ppm \cdot 10^{-6}$$

where s is the coil distance, $\omega = 2\pi f$ is the angular frequency for the frequency, f , and $\mu_0 = 4\pi \cdot 10^{-7}$. In order to calculate the uncertainty, data values for individual data point are converted from apparent resistivity to ppm by rewriting the equation above:

$$ppm_{m\grave{a}lt} = \frac{1,974 \cdot f \cdot s^2}{\rho_a}$$

Table 1 shows the added absolute uncertainty for each receiver coil configuration. A 3% uniform uncertainty has been added on top of that.

Receiver coil configuration	PRP1	HCP1	PRP2	HCP2	PRP4	HCP4
Uncertainty [ppm]	2.44	4.30	17.99	20.43	72.96	43.55

Table 1. Absolute uncertainty for each receiver coil configuration.

The total relative data uncertainty, $\Delta\rho_a$ for the individual data point is then:



$$\Delta\rho_a = \sqrt{0,03^2 + \left(\frac{ppm_{unc}}{ppm_{målt}}\right)^2}$$



6. INVERSION

Inversion and evaluation of inversion results are performed with Aarhus Workbench, which uses the inversion code AarhusInv, both have been developed by the HydroGeophysics Group, Aarhus University.

The data are inverted with a 1D SCI model setup. The settings for the inversion are shown in Table 2.

		Value
Software	Aarhus Workbench Version	5.3.1.0
Start model	Number of layers	10
	Start resistivity [Ωm]	40
	Layer thickness first layer [m]	0.2
	Depth to last layer [m]	10
	Distribution of layer thickness	Logarithmically rising with depth
SCI constraints	Horizontal constraints on resistivities [factor]	1.6
	Reference distance [m]	1
	GCM height above ground	30 cm
	Vertical constraints on resistivities [factor]	3.0
	Prior, thickness	Fixed
	Prior, resistivities	None
	Number of SCI cells	1

Table 2. Inversion settings, smooth SCI setup.

6.1 The SCI-method

The SCI inversion method (Spatially Constrained Inversion) uses constraint between the 1D model along as well as across the measurement lines (Figure 9). The inversion is a nonlinear damped least squares method where the instrument's transfer function is fully modelled to its known extent (filters, wave forms, geometry).

The instrument height is as a model parameter in the inversion and is routinely carried out for airborne measurements. For the GCM measurements we do not have actual measurements of the instrument height and thus this is fixed in the inversion.

The model parameters in the models of the SCI interpretation is tied to a distance dependent variance. The constraints between the measurements are tied together form Delaunay triangles (Figure 10), by which each measurement is tied to its 'best neighbors'. Delaunay triangulation always connect neighboring lines with the



primary function of breaking down the line orientation in the data. In this way, we can avoid matters where the inversion results are influenced by data measured in lines. By tying together the model parameters, we achieve a better resolution of resistivities and layer borders than by performing an inversion of each individual measurement.

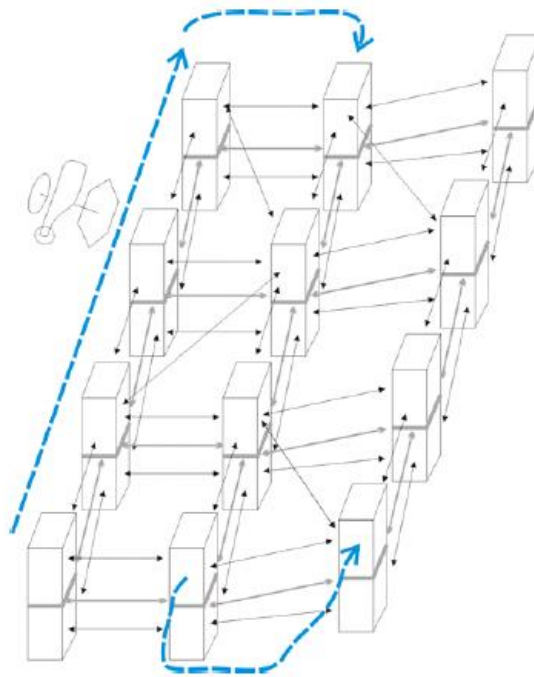


Figure 9. Schematic concept of an SCI inversion. In the inversion constraints are used along and across the driving lines.

An SCI inversion can be used for a few layer model (3-6 layers) with free parameters as well as for a many layer model (10-30 layers) with fixed thickness, but free resistivities. For a many layer model, vertical constraints are used between the layers in order to achieve a more stable inversion. Here only many layer models are used.

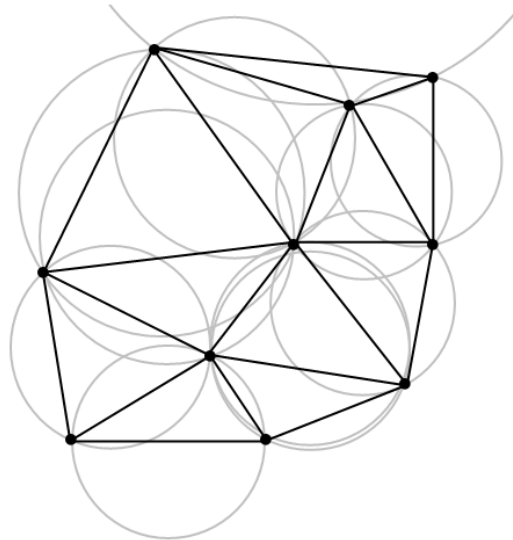


Figure 10. Example of Delaunay triangulation of points on one plane.

6.2 Depth of Investigation

For each model a conservative and standard DOI (Depth Of Investigation) is calculated, where system parameters, all data points and data uncertainties are considered. The model parts lying above the conservative DOI can be presumed to be well-founded in the data. Estimated values lying below the standard DOI should not be used for the interpretation of data, and values between the conservative and standard DOI can be used with caution.

The DOI is calculated from the calculated sensitivity matrix (Jacobian) from the final model. It is only data based and thus a priori information and constraints do not influence the calculation of the DOI. An example of DOI is shown in Figure 11 to the left where the sensitivity function is plotted based on a 3-layer model from a TEM sounding. The function is calculated from the sensitivity matrix and shows a higher sensitivity in layers with low resistivities (layer 1 and 3).

If you plot the integrated sensitivity function from the depth you will get the plot shown to the right in Figure 11. In this example, a DOI limit has been set at a cumulated sensitivity of 0,8. This means that there is not enough sensitivity below this depth for the information to be used for interpretation.

Conservative and standard DOI indicated in the Workbench are set at respectively 0,6 and 1,2. For GCM interpretations we use the standard DOI value as the limit.

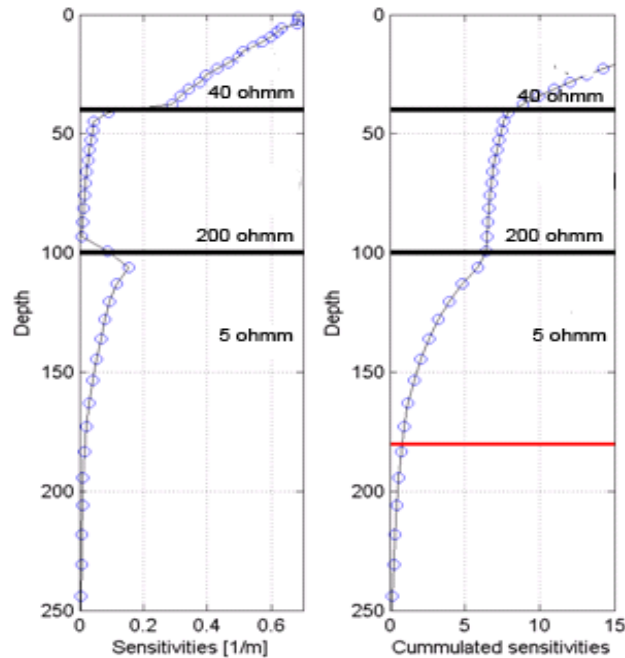


Figure 11. Calculated sensitivities for a 3-layer model performed with TEM. Left: the sensitivity function where the sensitivity is higher for the layers with low resistivities. Right: the integrated sensitivity function. De red line indicates DOI with a sensitivity of 0,8.

6.3 Mean-resistivity maps

The results from the inversion are 1D models describing depth intervals (layers) and the resistivities of each depth interval. For visualizing the results a mean-resistivity map is made, showing a calculated mean-resistivity of a given depth interval. The calculations for each model are shown in Figure 12, where [A,B] is the desired depth interval, [d0:d3] is the depth to the layer border, and [ρ_1 : ρ_4] are the resistivities for each layer. Here the desired depth interval is split into 3 thicknesses [Δt_1 : Δt_3] and the mean-resistivities are calculated by:

$$\rho_{vertical} = \frac{\rho_1 \cdot \Delta t_1 + \rho_2 \cdot \Delta t_2 + \rho_3 \cdot \Delta t_3}{\Delta t_1 + \Delta t_2 + \Delta t_3}$$

A general expression of the mean-resistivity in a given depth interval is:

$$\rho_{vertical} = \frac{\sum_{i=1}^n \rho_i \cdot \Delta t_i}{\sum_{i=1}^n \Delta t_i}$$



i goes from 1 to the number of thicknesses in the give depth interval. This calculated mean-resistivity equals the average resistivity if a current is sent vertically through the interval.

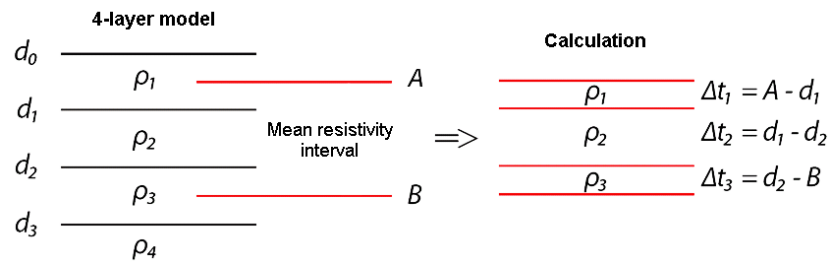


Figure 12. Calculation of mean-resistivity for the depth interval [A,B].

The mean-resistivity can also be calculated when the current is sent horizontally through the depth interval. This is called the horizontal mean-resistivity. It is calculated as the reciprocal mean conductivity σ_{mean} and is given by:

$$\rho_{horizontal} = \frac{1}{\sigma_{mean}} = \left[\frac{\sum_{i=1}^n \left(\frac{1}{\rho_i} \right) \cdot \Delta t_i}{\sum_{i=1}^n \Delta t_i} \right]^{-1}$$

Usually, the difference between these two calculated mean-resistivities is small, but the horizontal mean-resistivity emphasizes the lower resistivities, which are often those of most interest.

For the GCM data the mean-resistivity maps are calculated with a horizontal mean-resistivity. Kriging has been used for interpolation with a search radius of 30 m.



6. RESULTS

In the following, the results of the mapping is shown as quality control maps, raw resistivity data maps, magnetic susceptibility maps, mean-resistivity maps, and profiles.



6.1 Quality control maps

In the following quality control maps are shown.

Model Location and GCM Lines

This map shows the actual GCM lines. Grey dots mark where data are disregarded due to line turns or coupling. Black dots mark where data is kept and inverted to a resistivity model.

A relatively small amount of data is disregarded due to coupling, and the coupled data are primarily associated with one cable running through the northwestern field and along the sides of the roads.

Data Residual

The data residual tells how well the obtained resistivity models explain the recorded data (how well the data is fitted). The data residual values are normalized with the data standard deviation, so a data residual below one corresponds to a fit within one standard deviation.

The data residual map is for the smooth inversion result. Some areas have relatively high data residual values (between 1 to 2), this is primarily due to noise data, which again is associated to low signal ground responses (resistive ground). In general, the data residuals are as expected for this type of environment and geological setting.

Number of data points

This map shows the number of data points in use for each resistivity model. Few data points correlate to areas with a low signal level (resistive areas). In general, all data points are present for each measurement.

Depth of Investigation (DOI)

This map shows the DOI estimates for the smooth model inversion result. DOI maps in depths are included in the appendix. Both DOI standard and DOI conservative maps are presented.

Digital Terrain Model (DEM)

DEM based on the GPS measurements from the GCM equipment.



HydroGeophysics Group
AARHUS UNIVERSITY



GCM Gedved 2017

Location, GCM lines
Black: 1D model Grey: Discarded data

UTM 32N WGS84



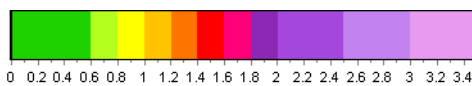
0.5 km



HydroGeophysics Group
AARHUS UNIVERSITY



GCM Gedved 2017



Data Residual
Below one corresponds to a fit within one standard deviation

UTM 32N WGS84

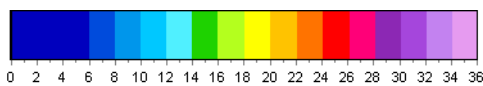




HydroGeophysics Group
AARHUS UNIVERSITY



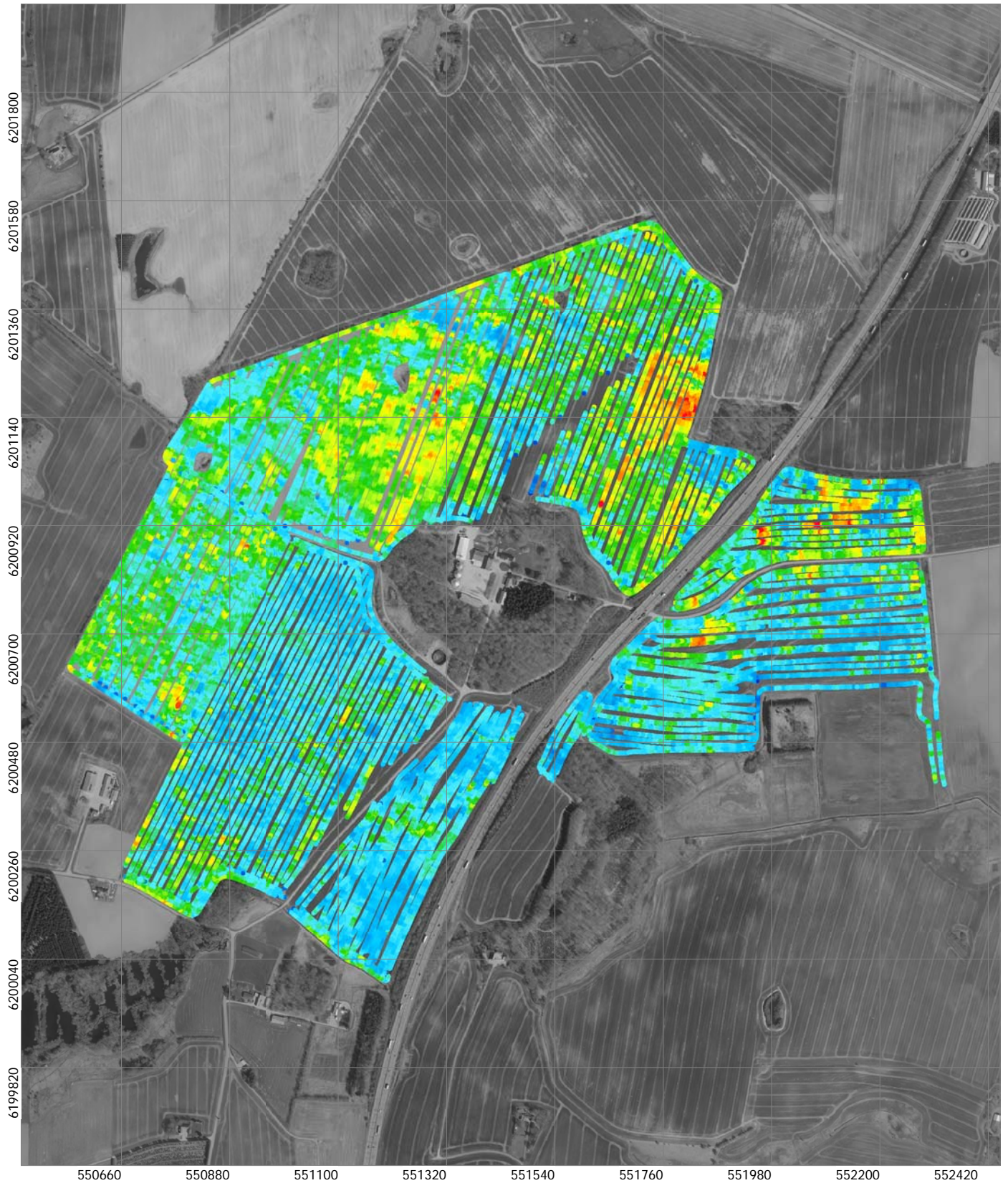
GCM Gedved 2017



Number of Datapoints
Datapoints used for inversion

UTM 32N WGS84

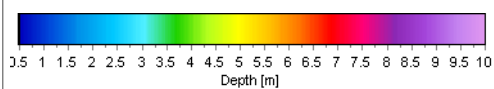




HydroGeophysics Group
AARHUS UNIVERSITY



GCM Gedved 2017



Depth of Investigation, Conservative
Depth, Meters

UTM 32N WGS84

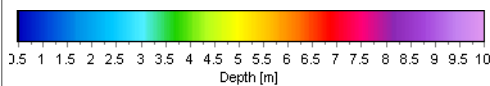




HydroGeophysics Group
AARHUS UNIVERSITY



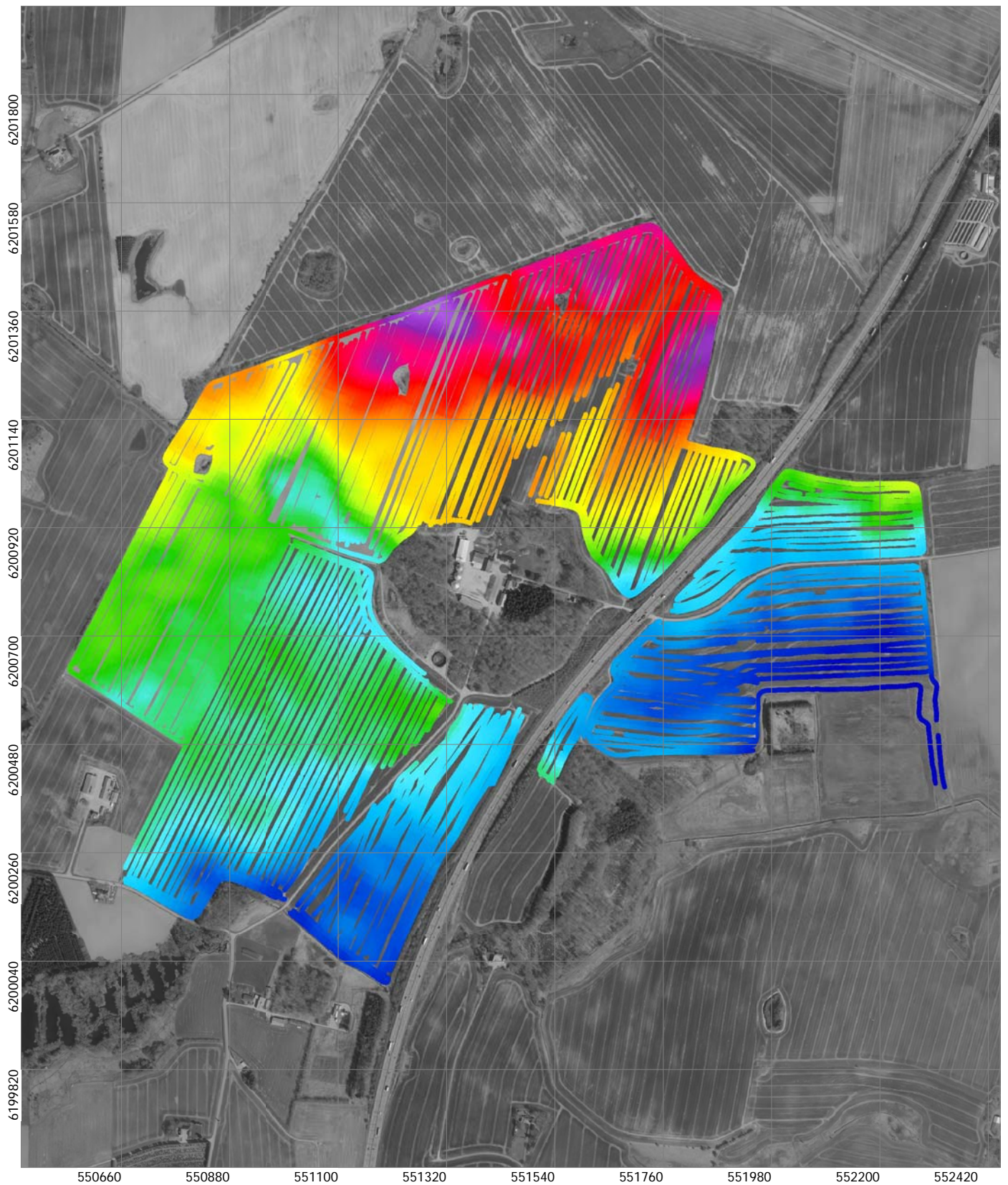
GCM Gedved 2017



Depth of Investigation, Standard
Depth, Meters

UTM 32N WGS84

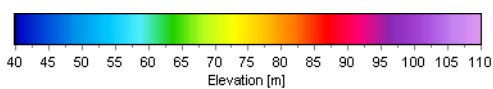




HydroGeophysics Group
AARHUS UNIVERSITY



GCM Gedved 2017



Digital Terrain Model
Elevation, Meters

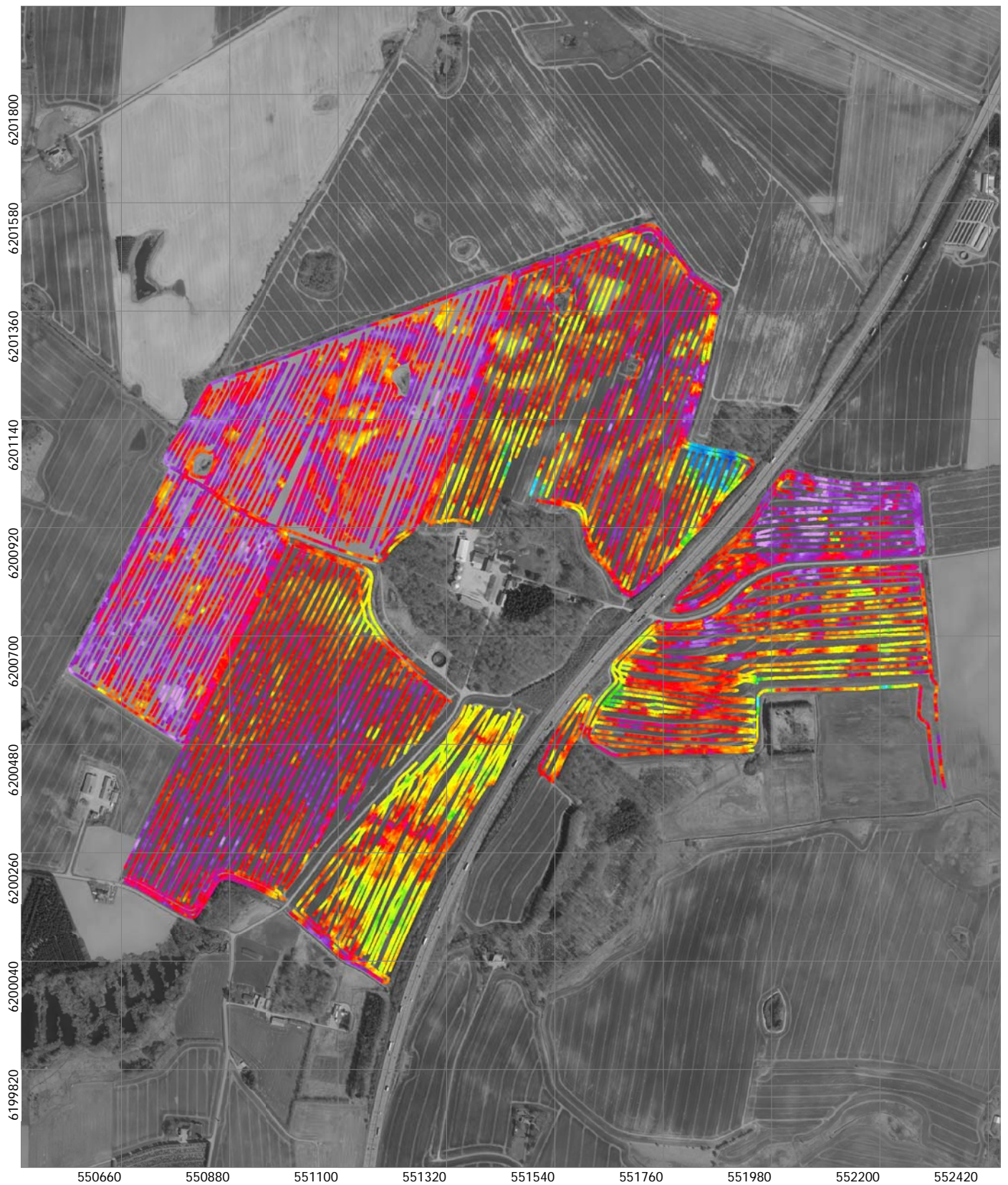
UTM 32N WGS84





6.2 Raw resistivity data maps

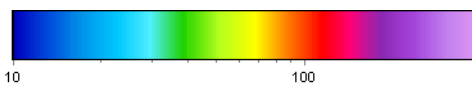
In the following raw resistivity data maps are shown for all six receiver configurations. Raw resistivity data measurements for the 6 different channels have been visualized as a point theme.



HydroGeophysics Group
AARHUS UNIVERSITY



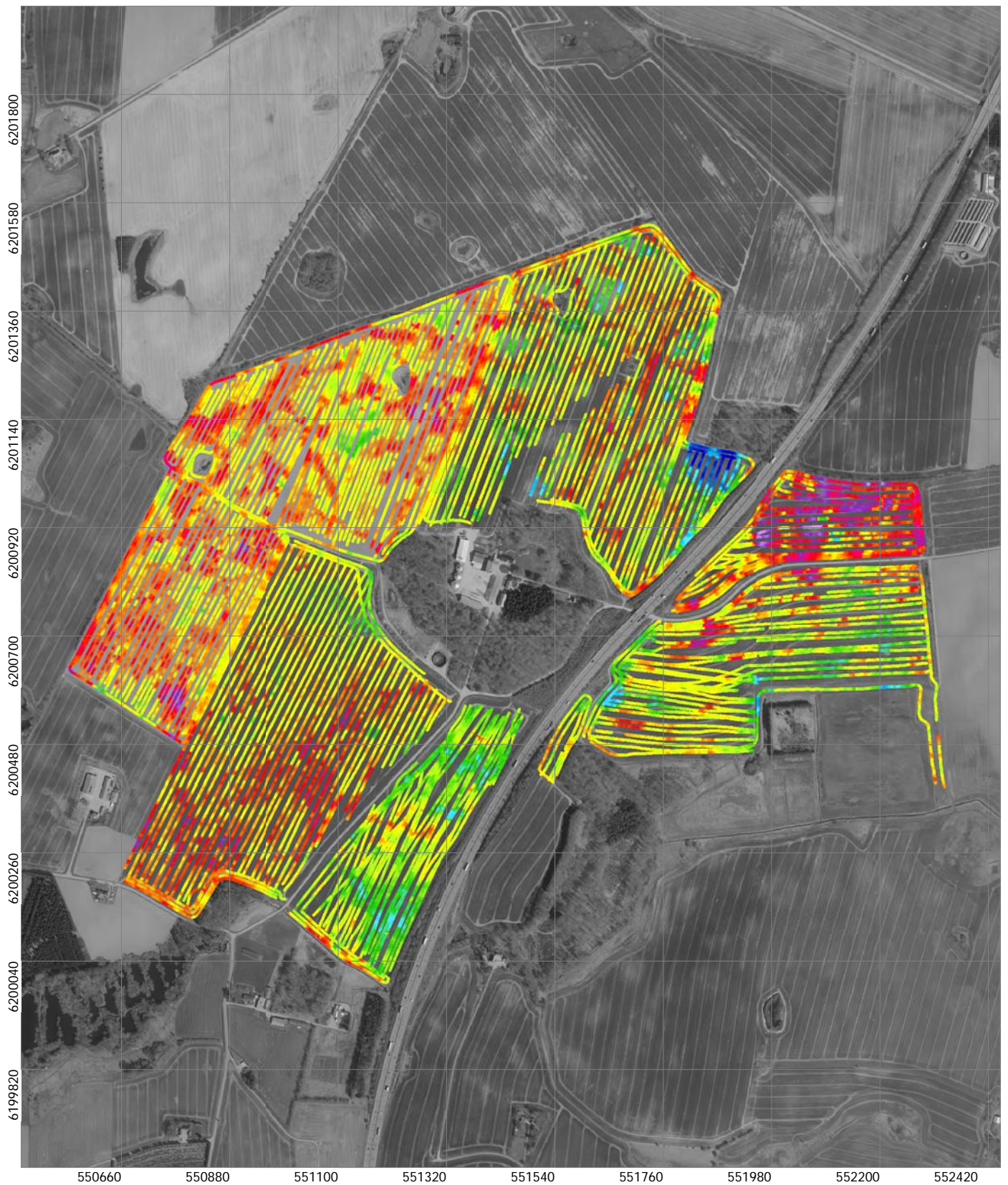
GCM Gedved 2017



PRP1 Receiver
Raw Resistivity Data - Point Theme

UTM 32N WGS84

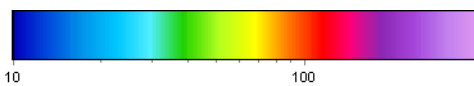




HydroGeophysics Group
AARHUS UNIVERSITY



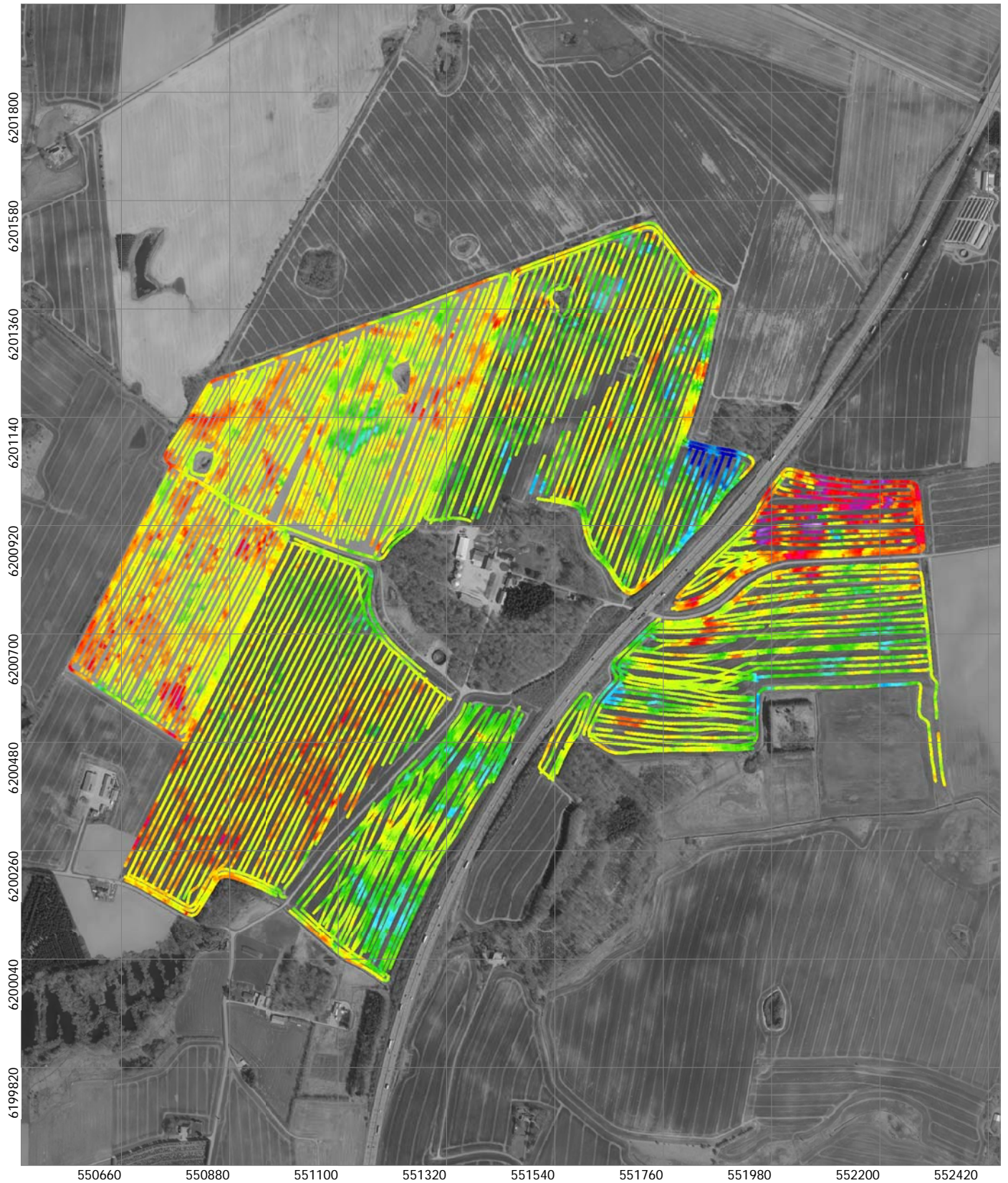
GCM Gedved 2017



PRP2 Receiver
Raw Resistivity Data - Point Theme

UTM 32N WGS84

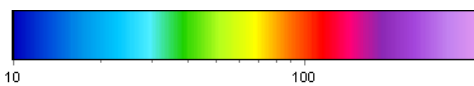




HydroGeophysics Group
AARHUS UNIVERSITY



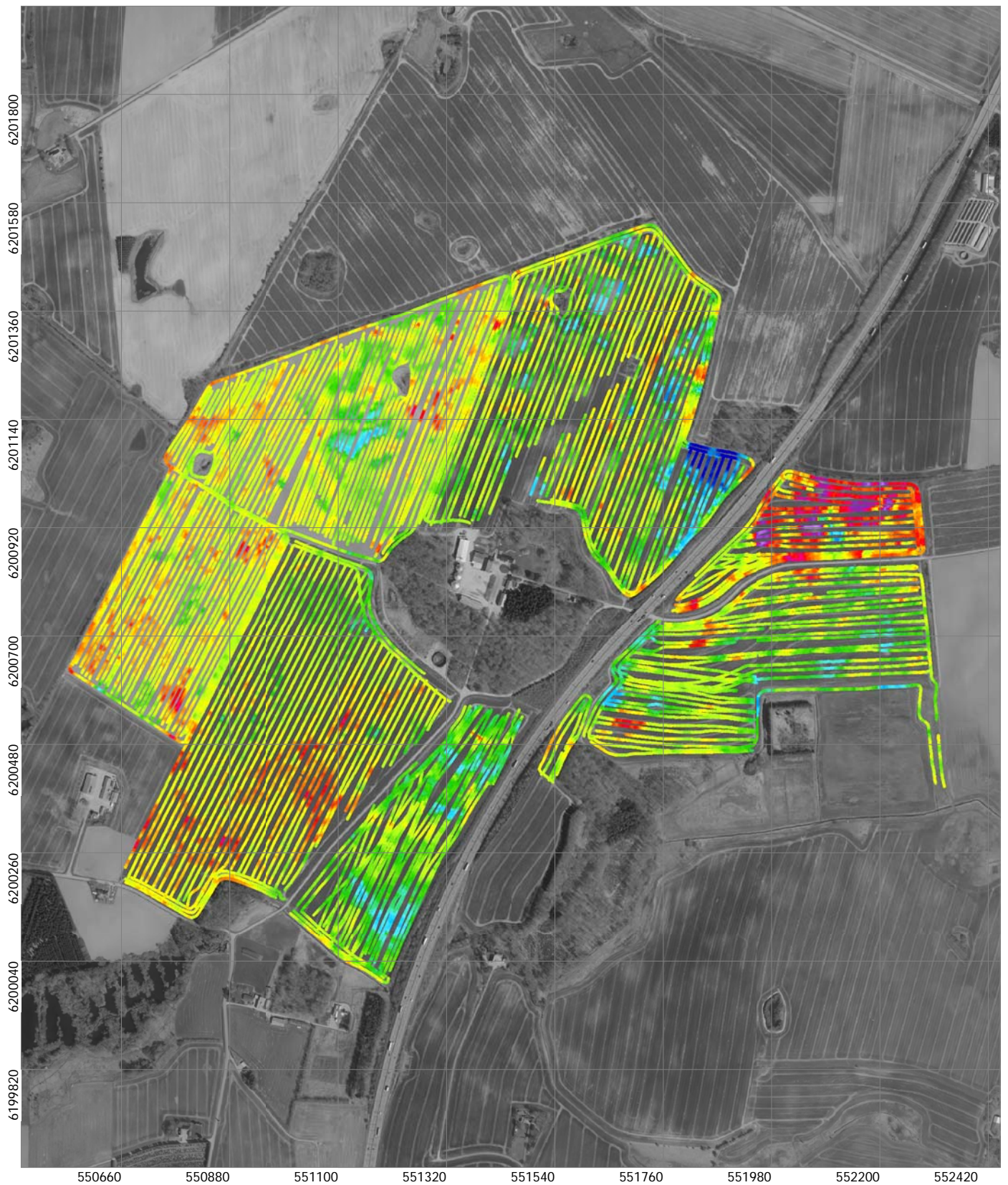
GCM Gedved 2017



HCP1 Receiver
Raw Resistivity Data - Point Theme

UTM 32N WGS84

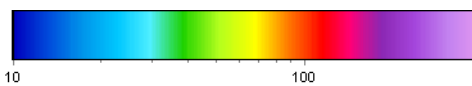




HydroGeophysics Group
AARHUS UNIVERSITY



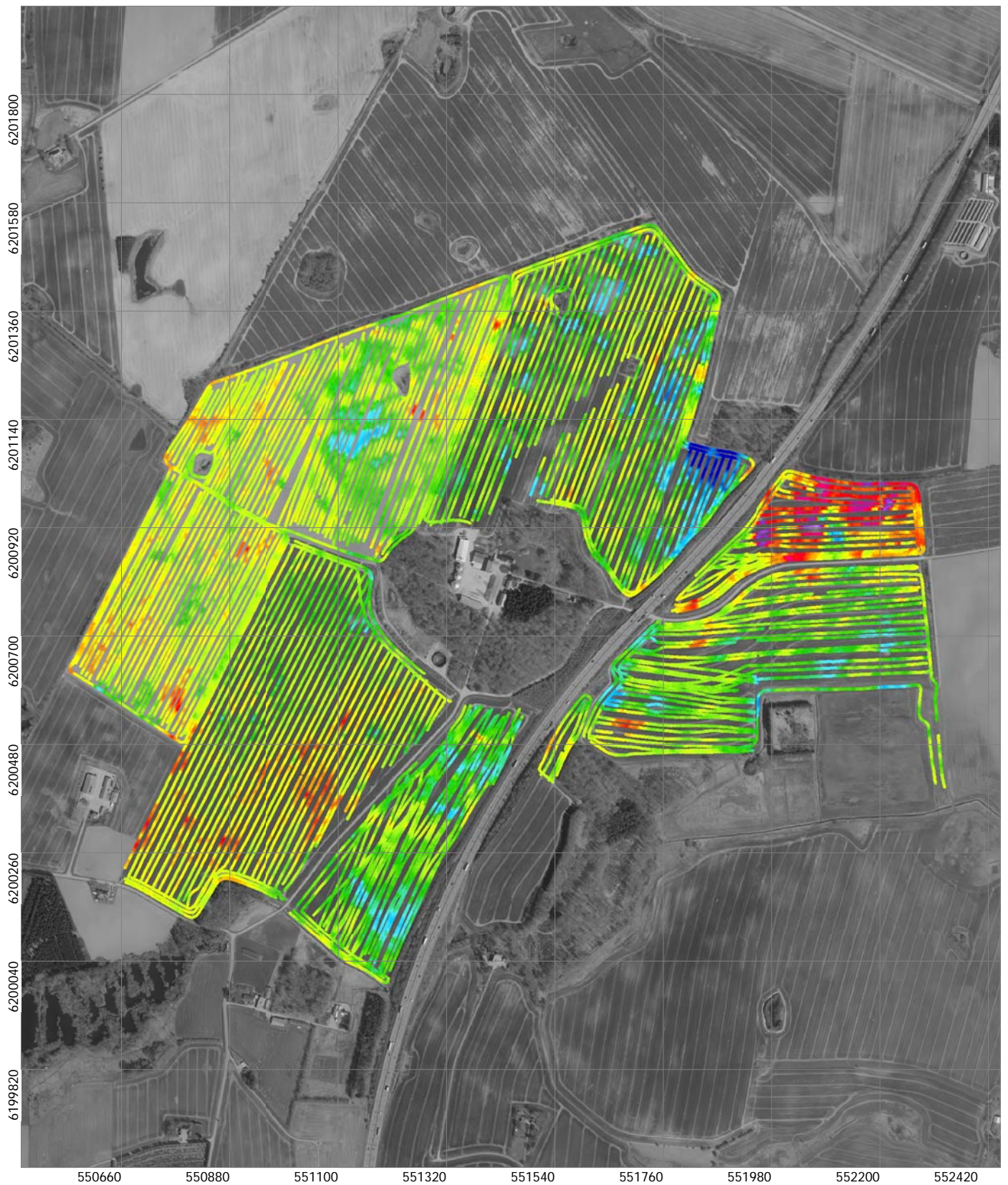
GCM Gedved 2017



PRP4 Receiver
Raw Resistivity Data - Point Theme

UTM 32N WGS84

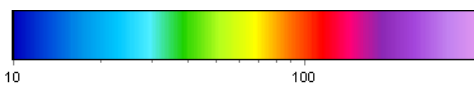




HydroGeophysics Group
AARHUS UNIVERSITY



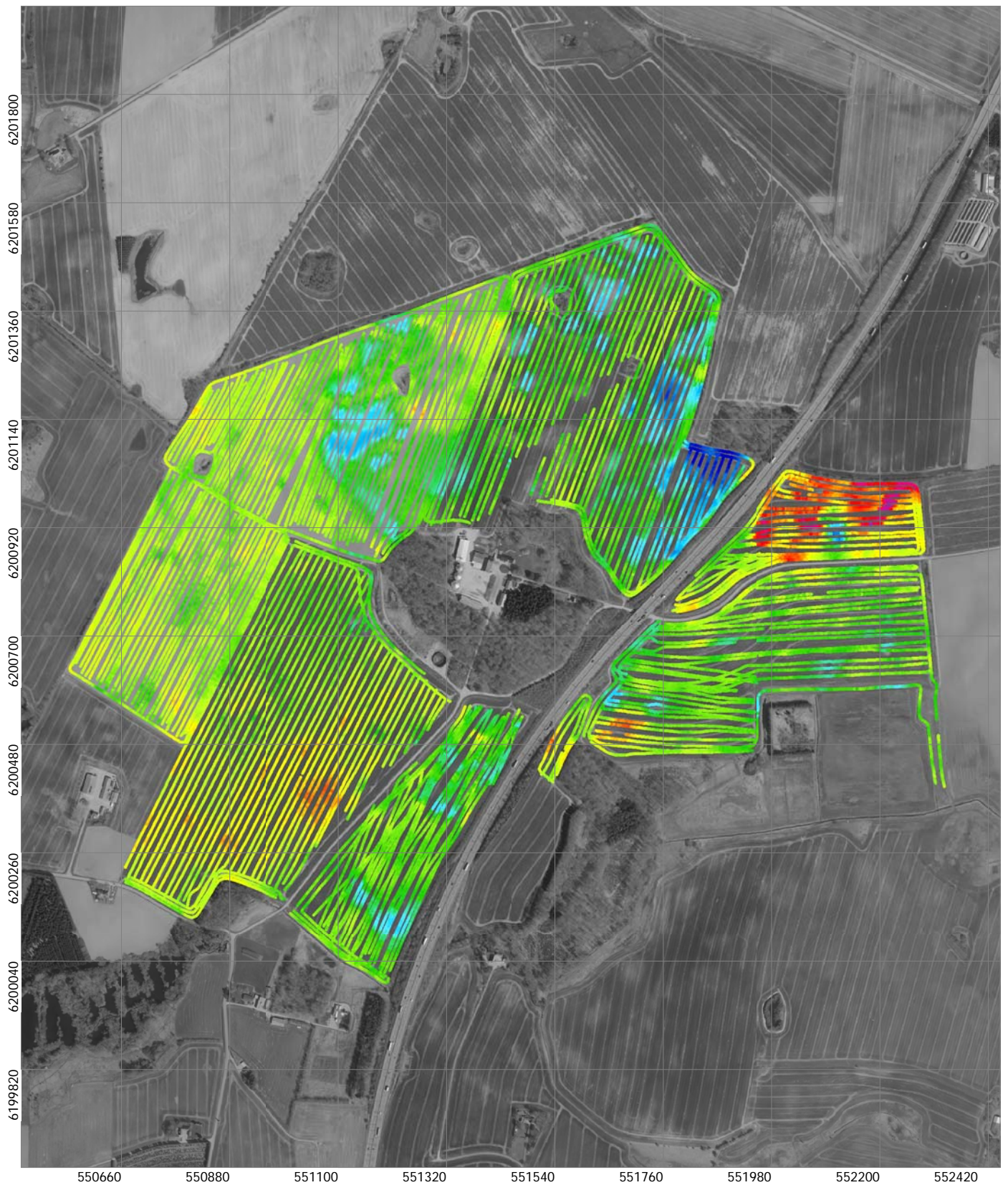
GCM Gedved 2017



HCP2 Receiver
Raw Resistivity Data - Point Theme

UTM 32N WGS84

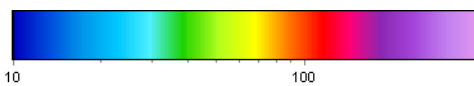




HydroGeophysics Group
AARHUS UNIVERSITY



GCM Gedved 2017



HCP4 Receiver
Raw Resistivity Data - Point Theme

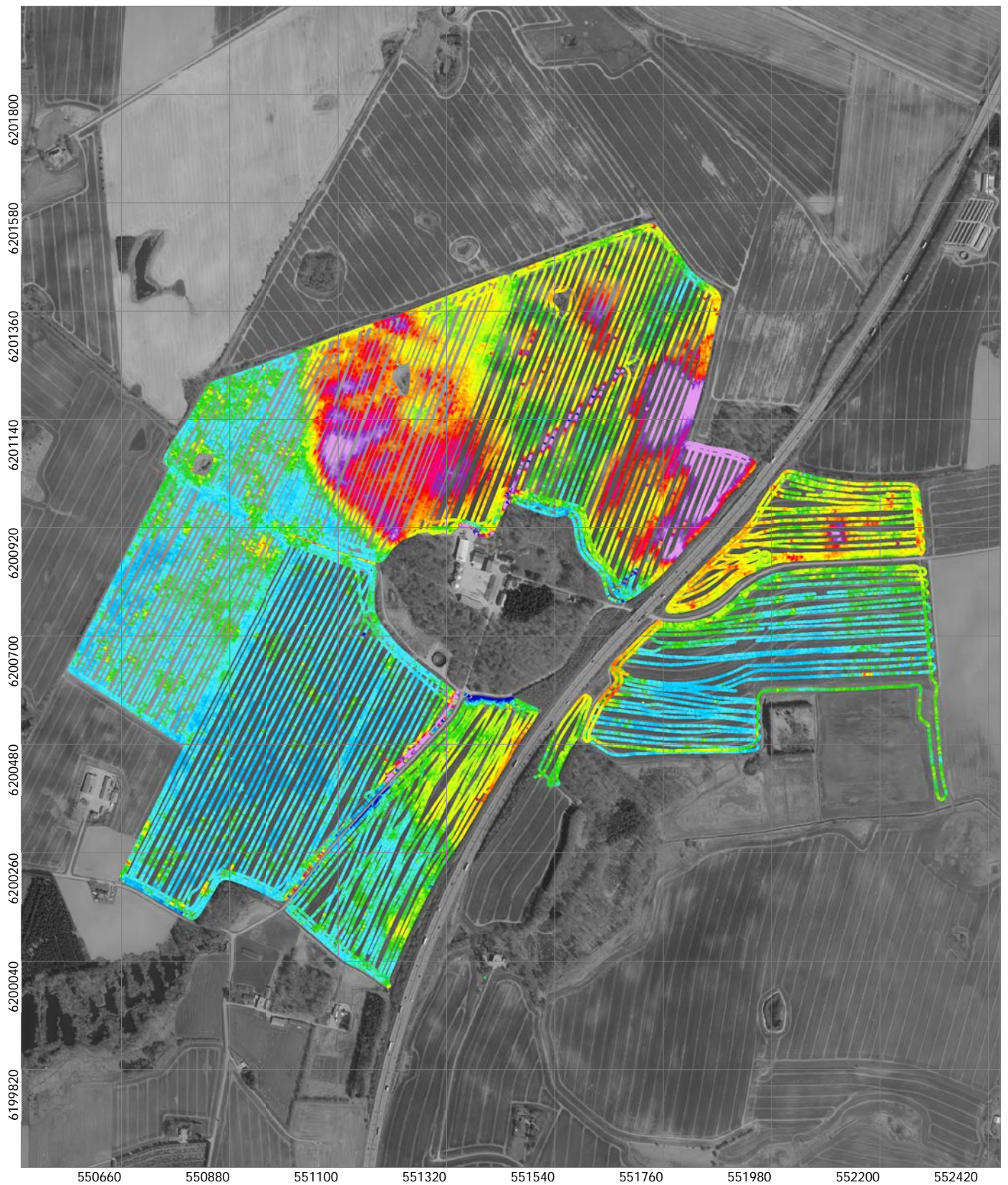
UTM 32N WGS84





6.3 Magnetic susceptibility

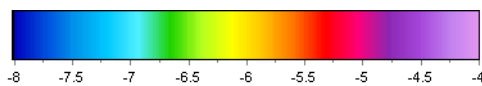
Magnetic susceptibility is a measure of whether a material can be magnetized. In relation to the emitted magnetic field from the DUALEM421 instrument. The magnetic susceptibility measurements are visualized as a point theme.



HydroGeophysics Group
AARHUS UNIVERSITY



GCM Gedved 2017



Magnetic Susceibility
Raw readings - Point theme

UTM 32N WGS84





6.4 Mean Resistivity

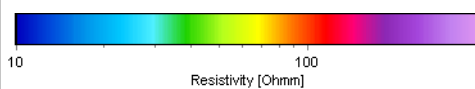
In the following mean-resistivity maps are shown. Mean-resistivity maps have been produced with 0.5 m intervals from a depth of 0 to 2 m and in 1 m intervals from a depth of 2 to 7 m. In the calculation of the mean-resistivity maps the standard DOI limit is used as the cutting line, and model information below this limit is not included.



HydroGeophysics Group
AARHUS UNIVERSITY



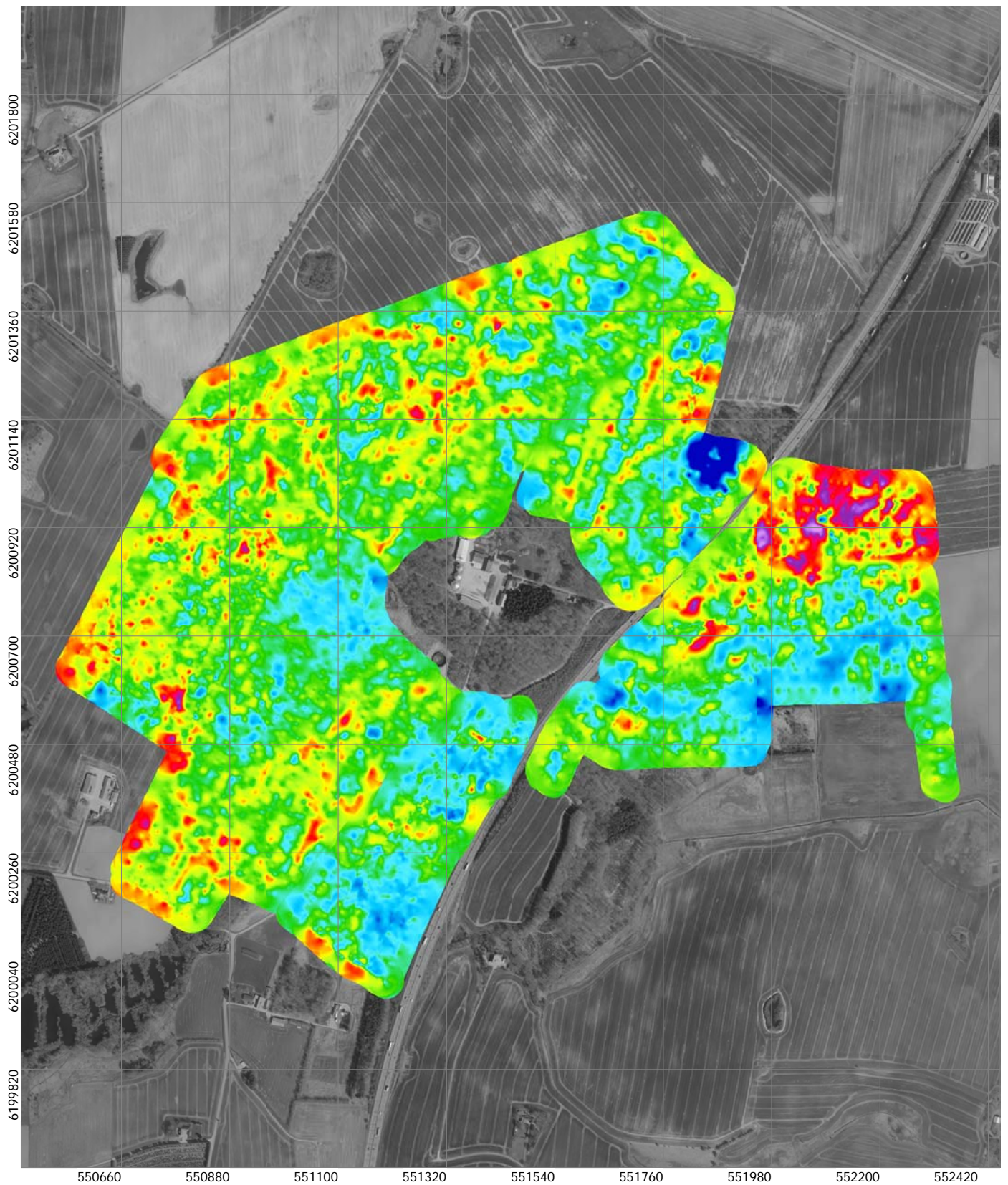
GCM Gedved 2017



Mean Resistivity - Depth 0 m - 0.5 m (ohm-m)
SCI Smooth Model - Kriging Search Radius 30 m

UTM 32N WGS84

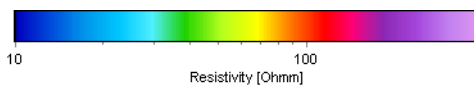




HydroGeophysics Group
AARHUS UNIVERSITY



GCM Gedved 2017



Mean Resistivity - Depth 0.5 m - 1.0 m (ohm-m)
SCI Smooth Model - Kriging Search Radius 30 m

UTM 32N WGS84

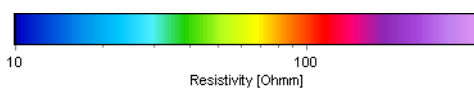




HydroGeophysics Group
AARHUS UNIVERSITY



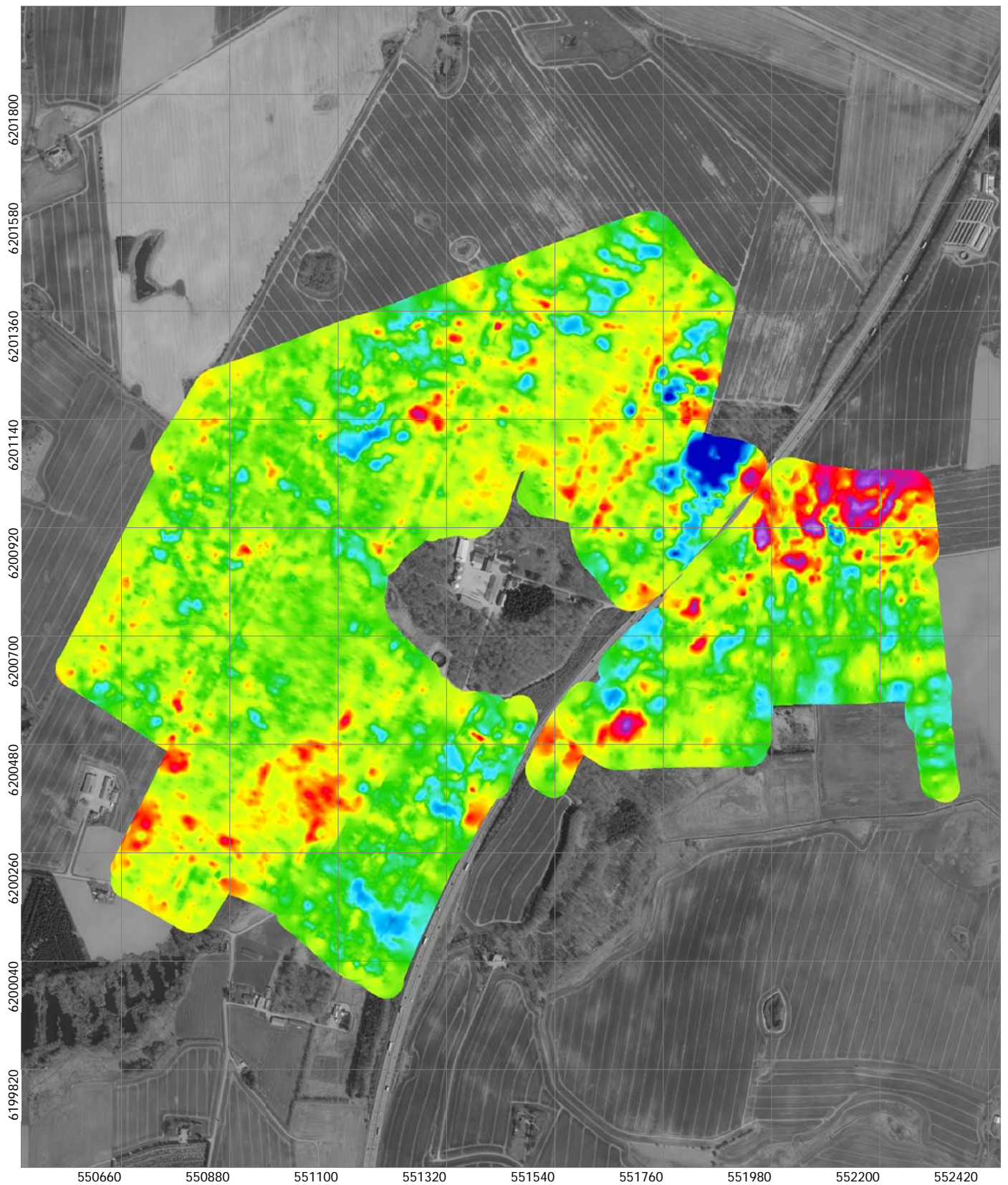
GCM Gedved 2017



Mean Resistivity - Depth 1.0 m - 1.5 m (ohm-m)
SCI Smooth Model - Kriging Search Radius 30 m

UTM 32N WGS84

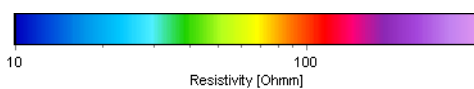




HydroGeophysics Group
AARHUS UNIVERSITY



GCM Gedved 2017



Mean Resistivity - Depth 1.5 m - 2.0 m (ohm-m)
SCI Smooth Model - Kriging Search Radius 30 m

UTM 32N WGS84

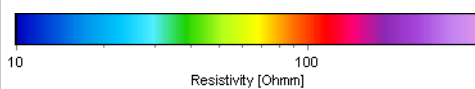




HydroGeophysics Group
AARHUS UNIVERSITY



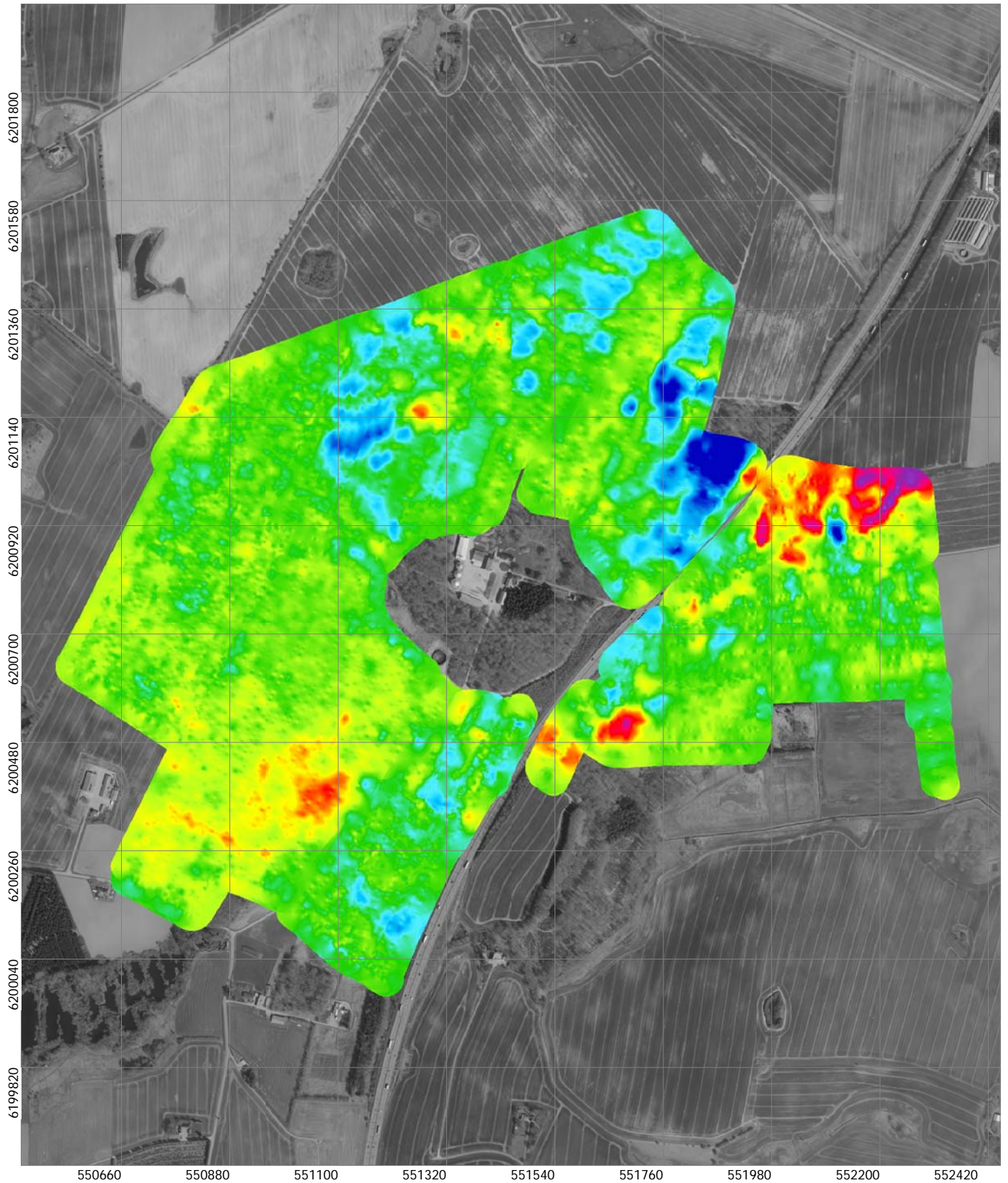
GCM Gedved 2017



Mean Resistivity - Depth 2.0 m - 3.0 m (ohm-m)
SCI Smooth Model - Kriging Search Radius 30 m

UTM 32N WGS84

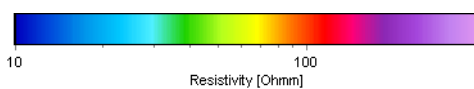




HydroGeophysics Group
AARHUS UNIVERSITY



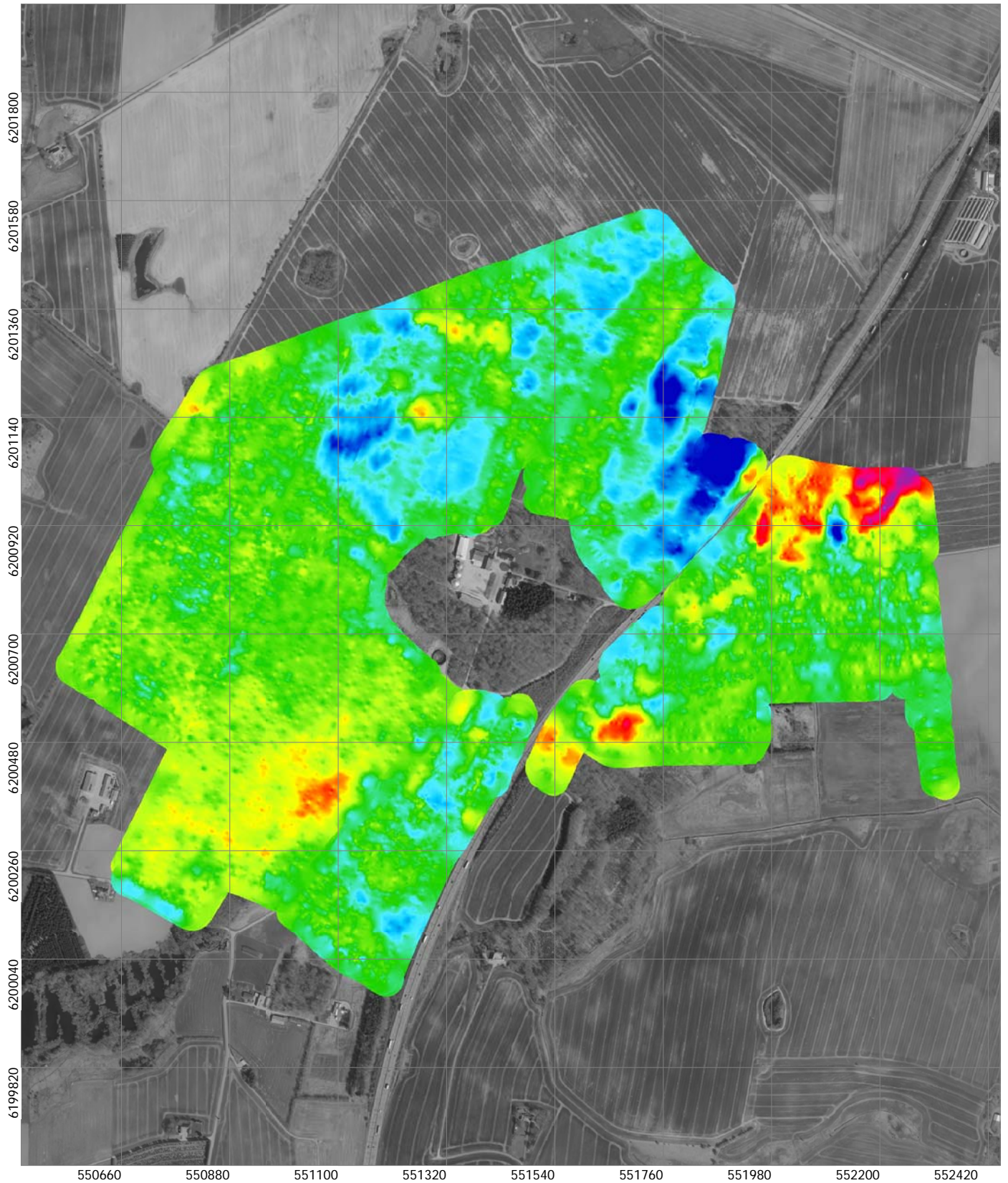
GCM Gedved 2017



Mean Resistivity - Depth 3.0 m - 4.0 m (ohm-m)
SCI Smooth Model - Kriging Search Radius 30 m

UTM 32N WGS84

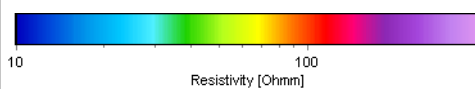




HydroGeophysics Group
AARHUS UNIVERSITY



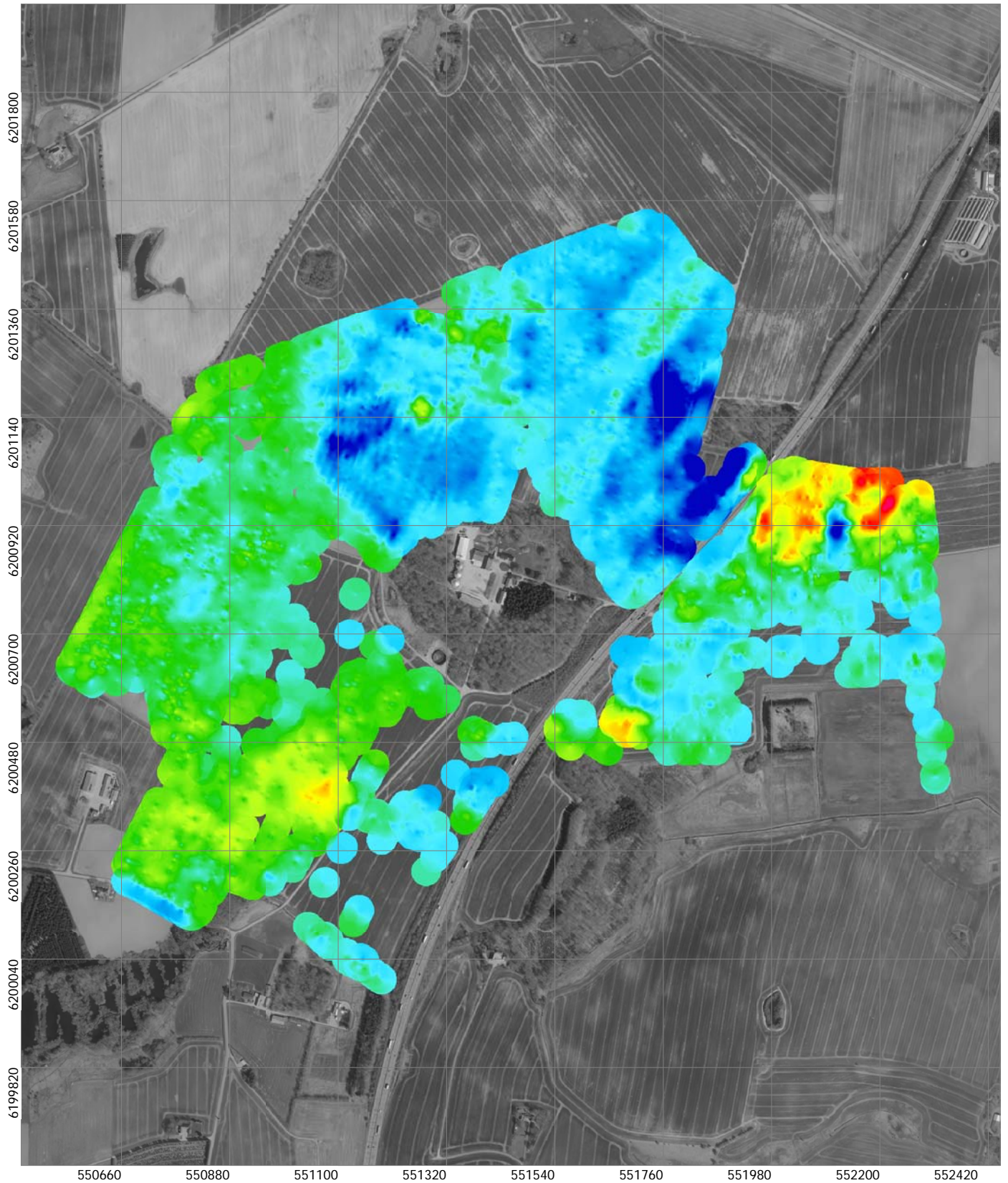
GCM Gedved 2017



Mean Resistivity - Depth 4.0 m - 5.0 m (ohm-m)
SCI Smooth Model - Kriging Search Radius 30 m

UTM 32N WGS84

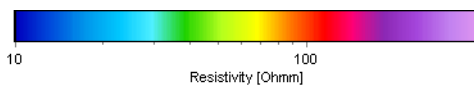




HydroGeophysics Group
AARHUS UNIVERSITY



GCM Gedved 2017



Mean Resistivity - Depth 6.0 m - 7.0 m (ohm-m)
SCI Smooth Model - Kriging Search Radius 30 m

UTM 32N WGS84



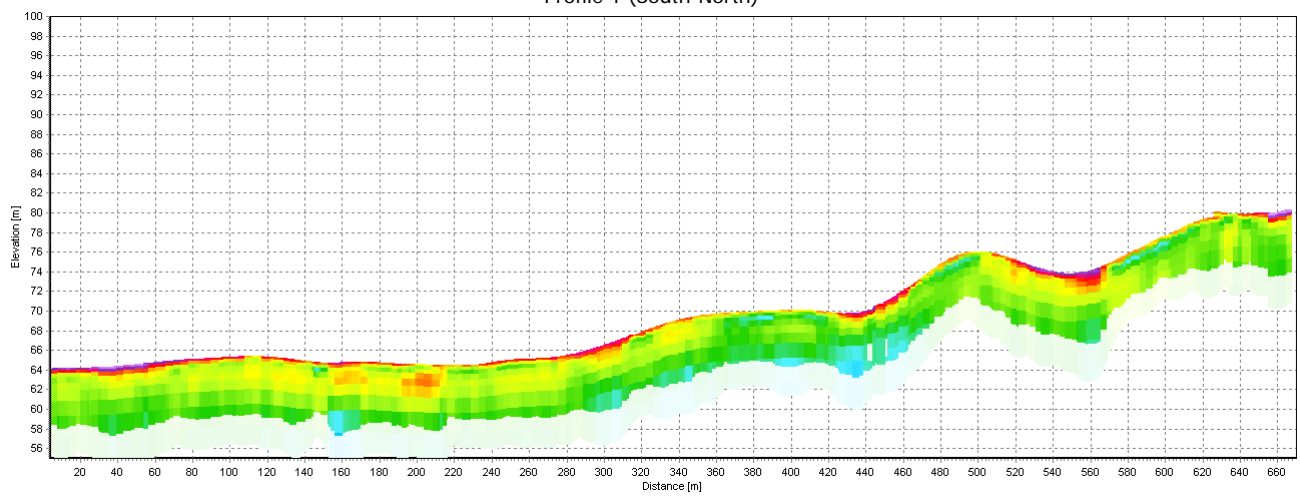


6.5 Profiles

In the profiles, the smooth inversion results is shown as models bars. The colors below the standard DOI limit are faded. Borehole information has been added to the profiles of the borehole are within a search radius of 10 meters from the profile.



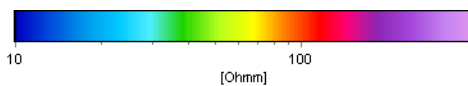
Profile 1 (South-North)



HydroGeophysics Group
AARHUS UNIVERSITY

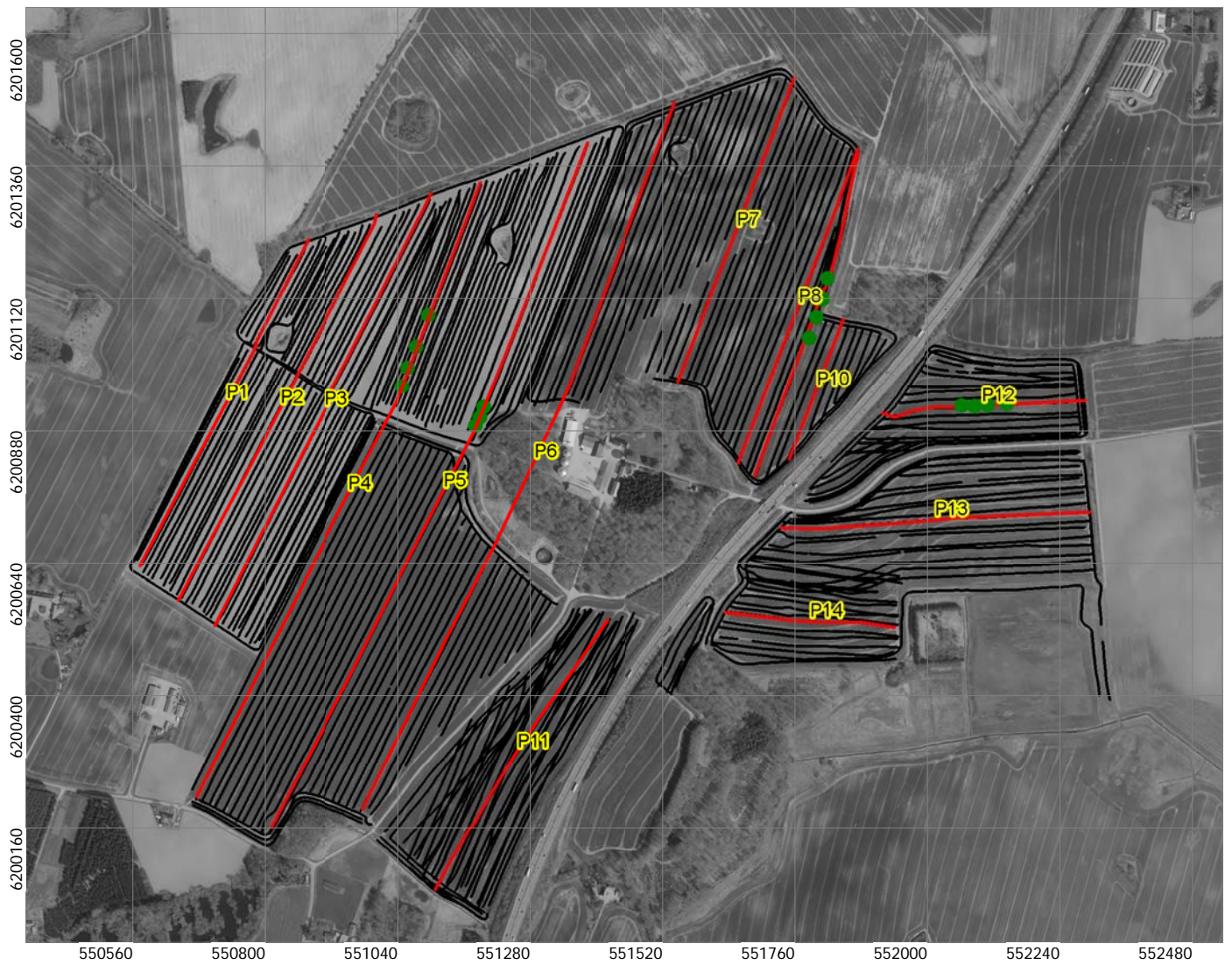


GCM Gedved 2017

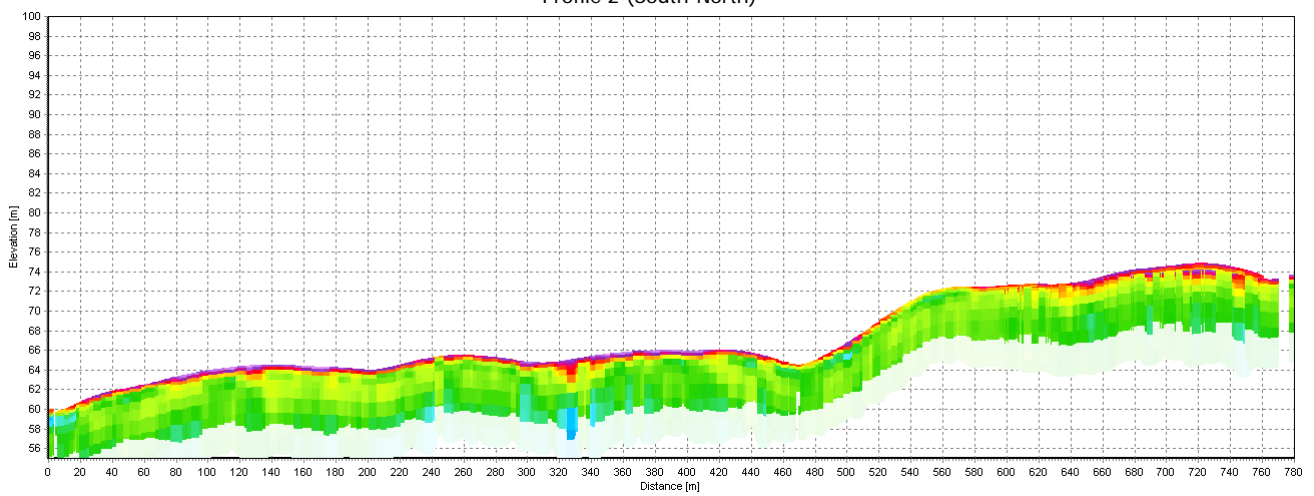


Resistivity Profiles (ohmm)
Smooth SCI Model

The profiles display model bars from the smooth inversion results
Models have been blanked by 75% below the DOI Standard



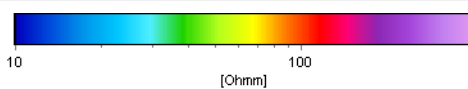
Profile 2 (South-North)



HydroGeophysics Group
AARHUS UNIVERSITY



GCM Gedved 2017

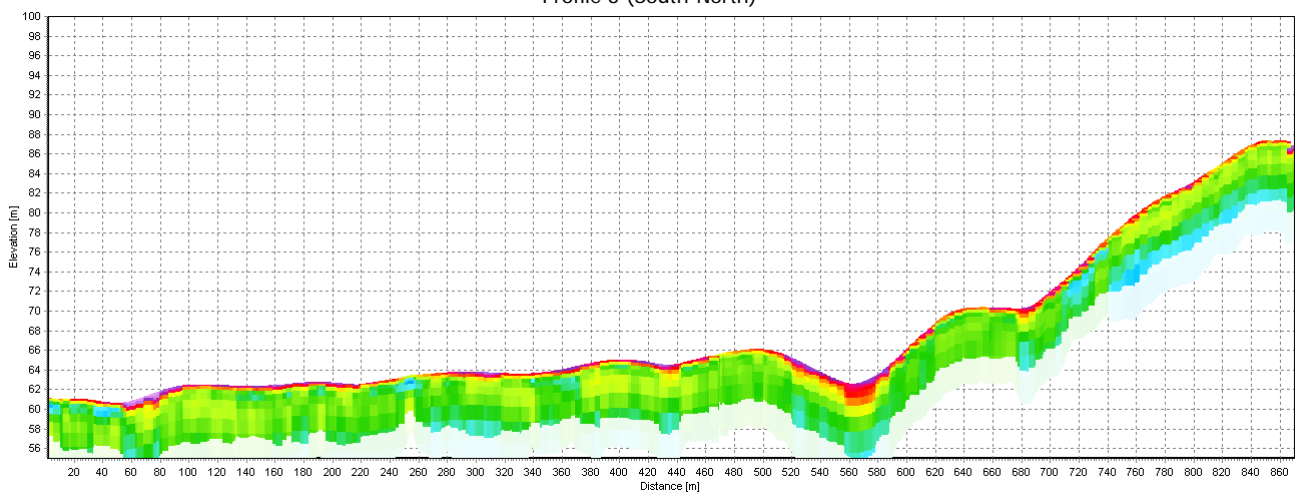


Resistivity Profiles (ohmm)
Smooth SCI Model

The profiles display model bars from the smooth inversion results
Models have been blanked by 75% below the DOI Standard



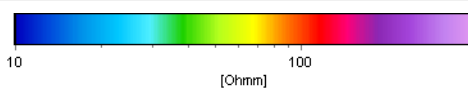
Profile 3 (South-North)



HydroGeophysics Group
AARHUS UNIVERSITY



GCM Gedved 2017

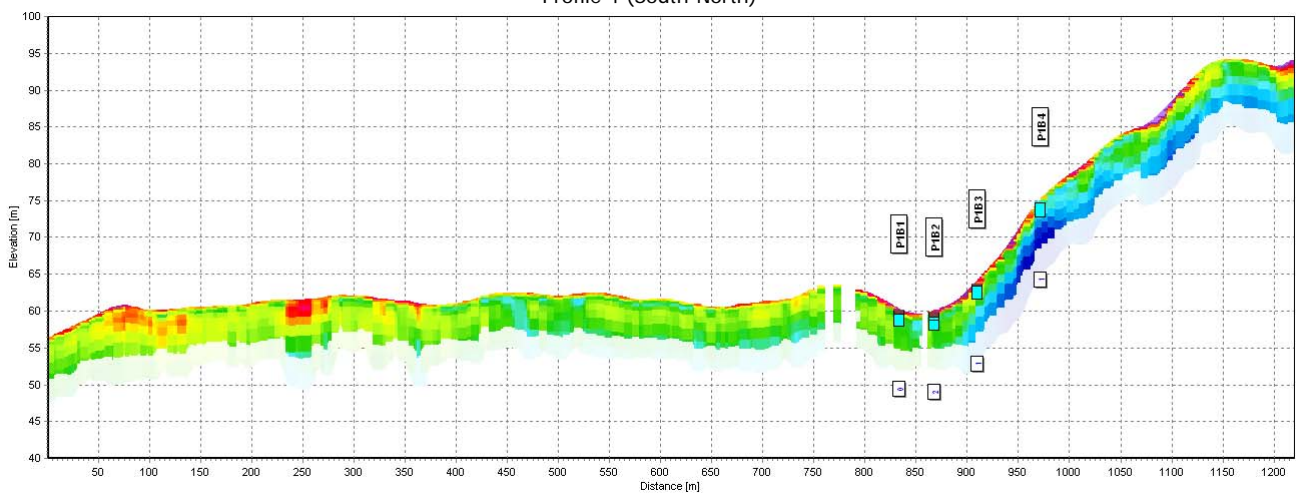


Resistivity Profiles (ohmm)
Smooth SCI Model

The profiles display model bars from the smooth inversion results
Models have been blanked by 75% below the DOI Standard



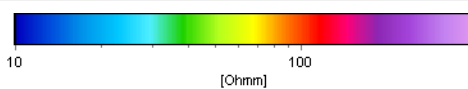
Profile 4 (South-North)



HydroGeophysics Group
AARHUS UNIVERSITY



GCM Gedved 2017



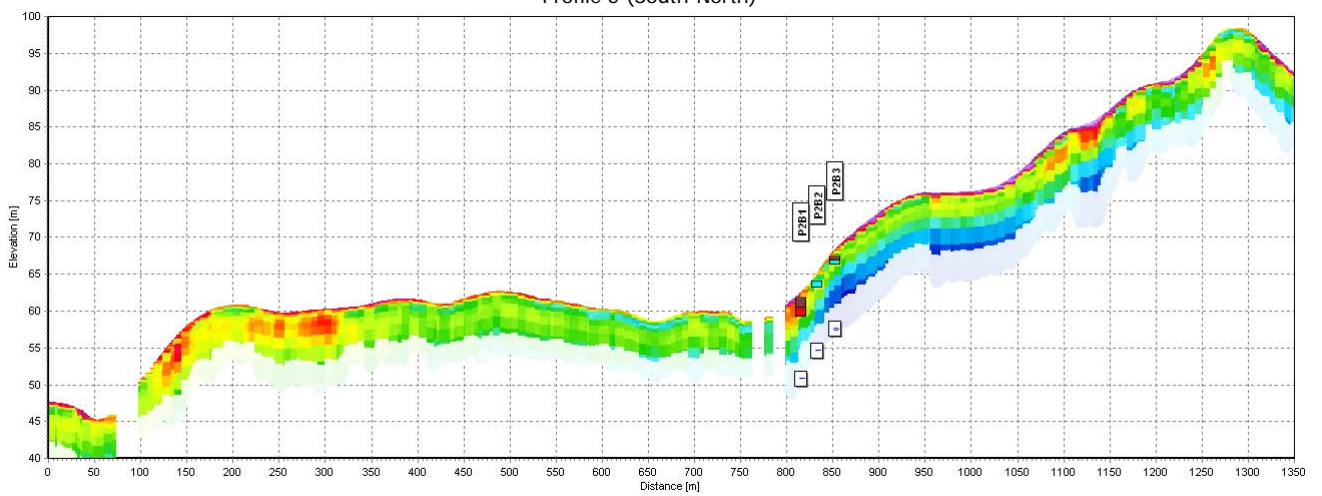
Resistivity Profiles (ohmm)

Smooth SCI Model

The profiles display model bars from the smooth inversion results
Models have been blanked by 75% below the DOI Standard
Borehole information - Blue:Clay Brown:Plowlayer Red:Sand



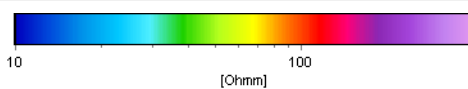
Profile 5 (South-North)



HydroGeophysics Group
AARHUS UNIVERSITY



GCM Gedved 2017



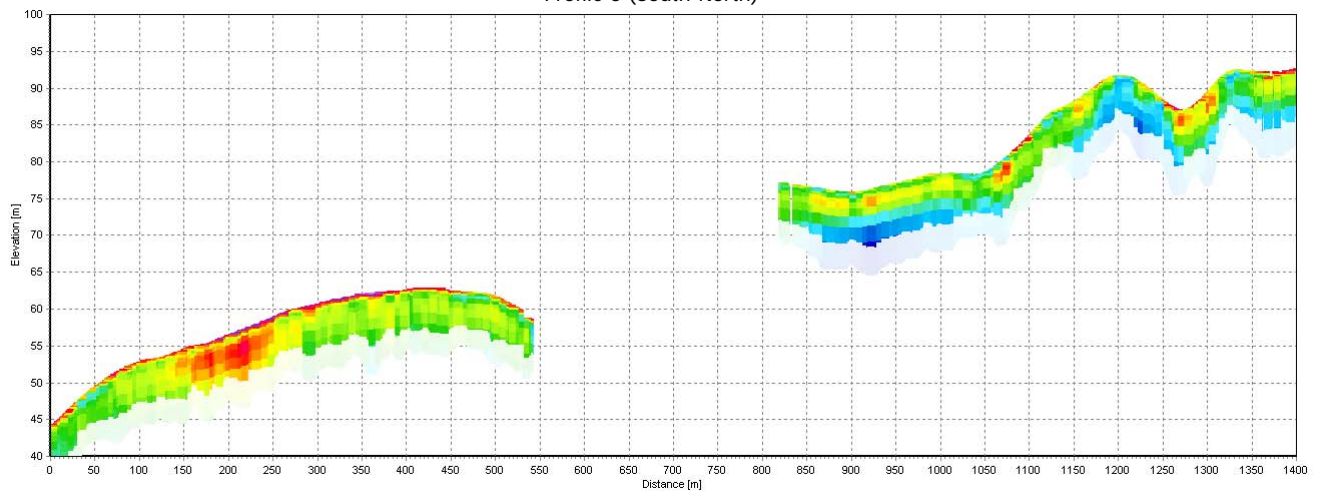
Resistivity Profiles (ohmm)

Smooth SCI Model

The profiles display model bars from the smooth inversion results. Models have been blanked by 75% below the DOI Standard Borehole information - Blue:Clay Brown:Plowlayer Red:Sand



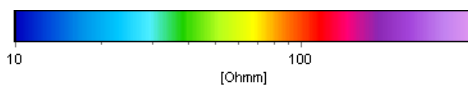
Profile 6 (South-North)



HydroGeophysics Group
AARHUS UNIVERSITY



GCM Gedved 2017

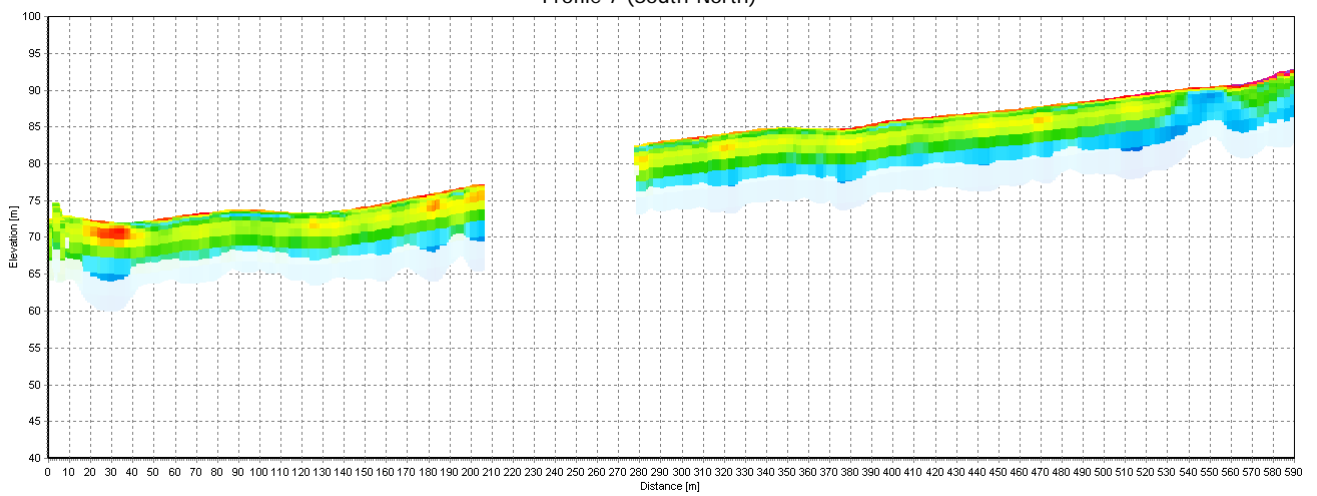


Resistivity Profiles (ohmm)
Smooth SCI Model

The profiles display model bars from the smooth inversion results
Models have been blanked by 75% below the DOI Standard



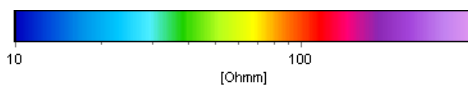
Profile 7 (South-North)



HydroGeophysics Group
AARHUS UNIVERSITY

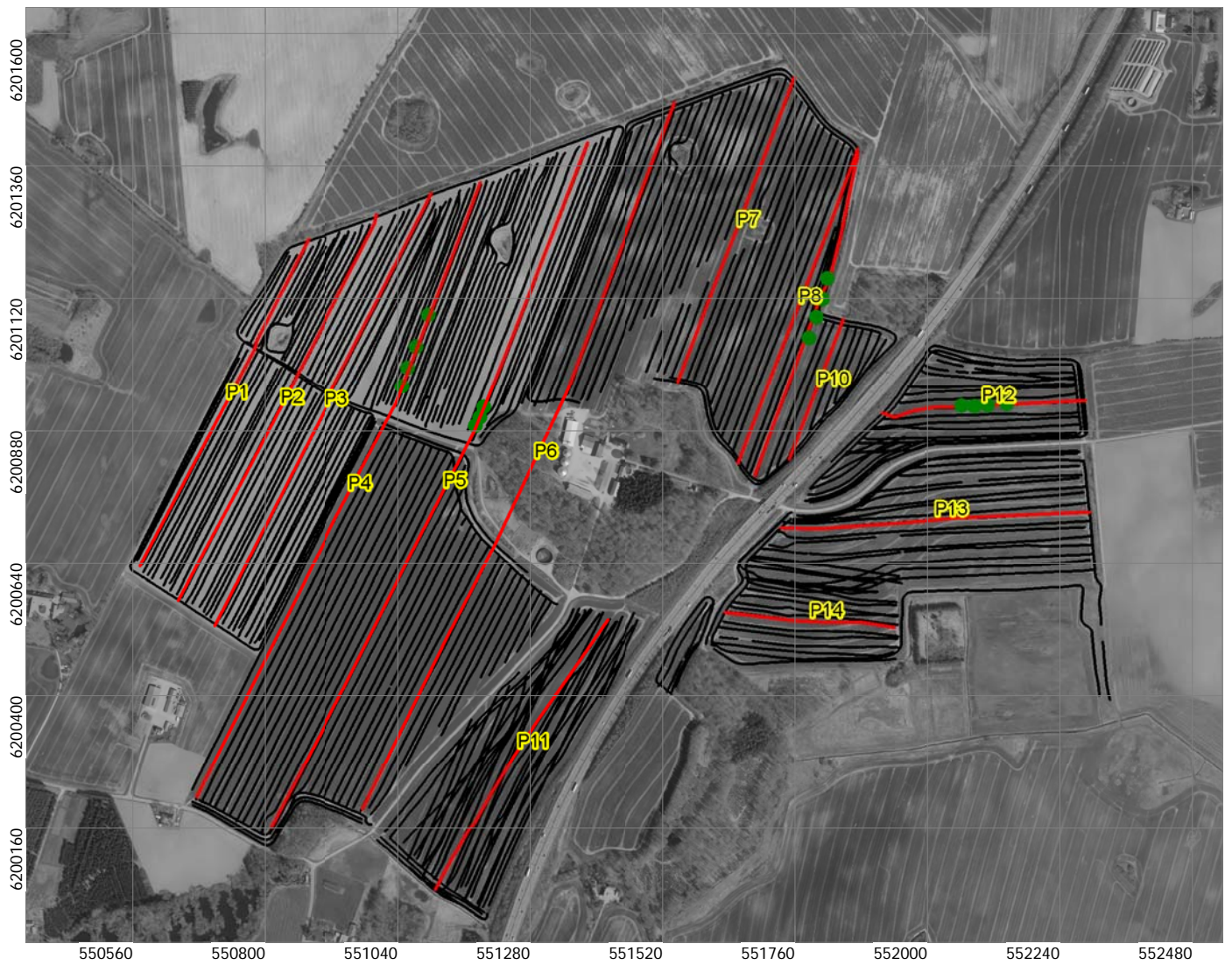


GCM Gedved 2017

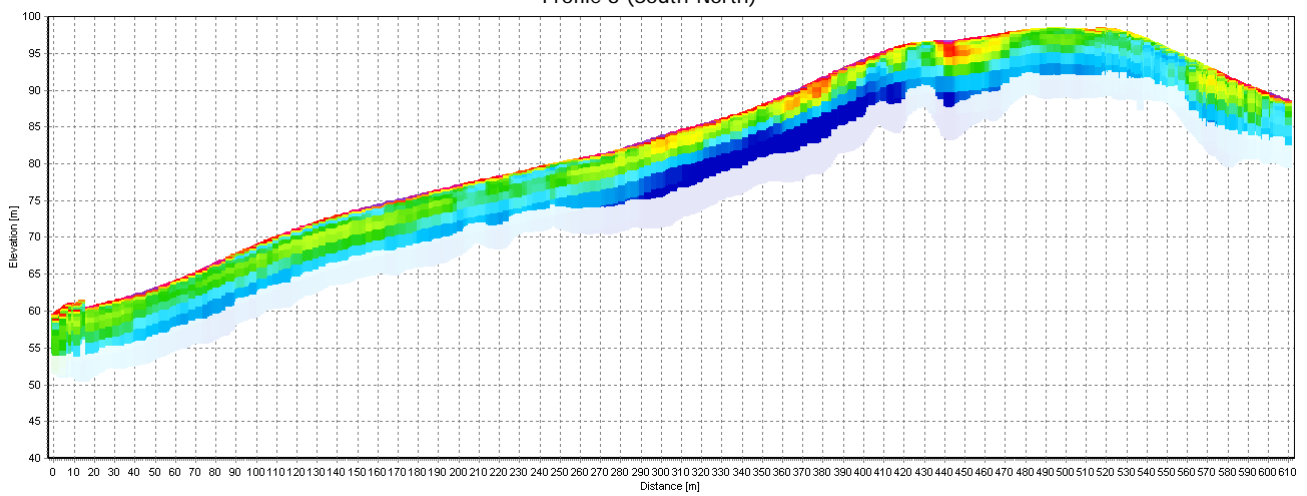


Resistivity Profiles (ohmm)
Smooth SCI Model

The profiles display model bars from the smooth inversion results
Models have been blanked by 75% below the DOI Standard



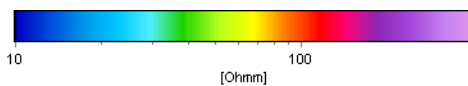
Profile 8 (South-North)



HydroGeophysics Group
AARHUS UNIVERSITY



GCM Gedved 2017

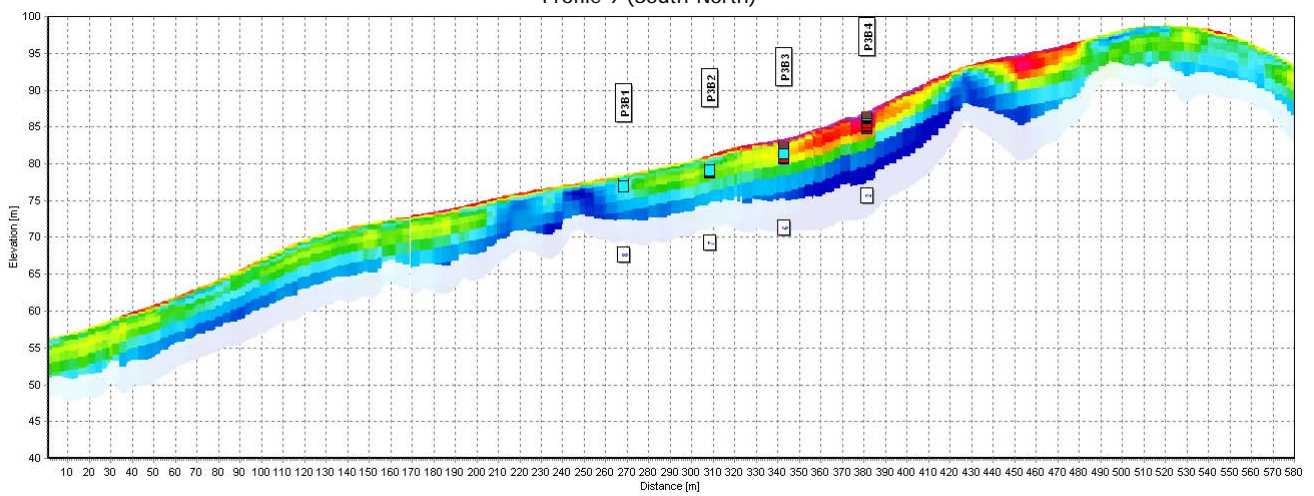


Resistivity Profiles (ohmm)
Smooth SCI Model

The profiles display model bars from the smooth inversion results
Models have been blanked by 75% below the DOI Standard



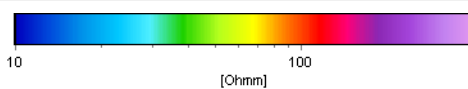
Profile 9 (South-North)



HydroGeophysics Group
AARHUS UNIVERSITY

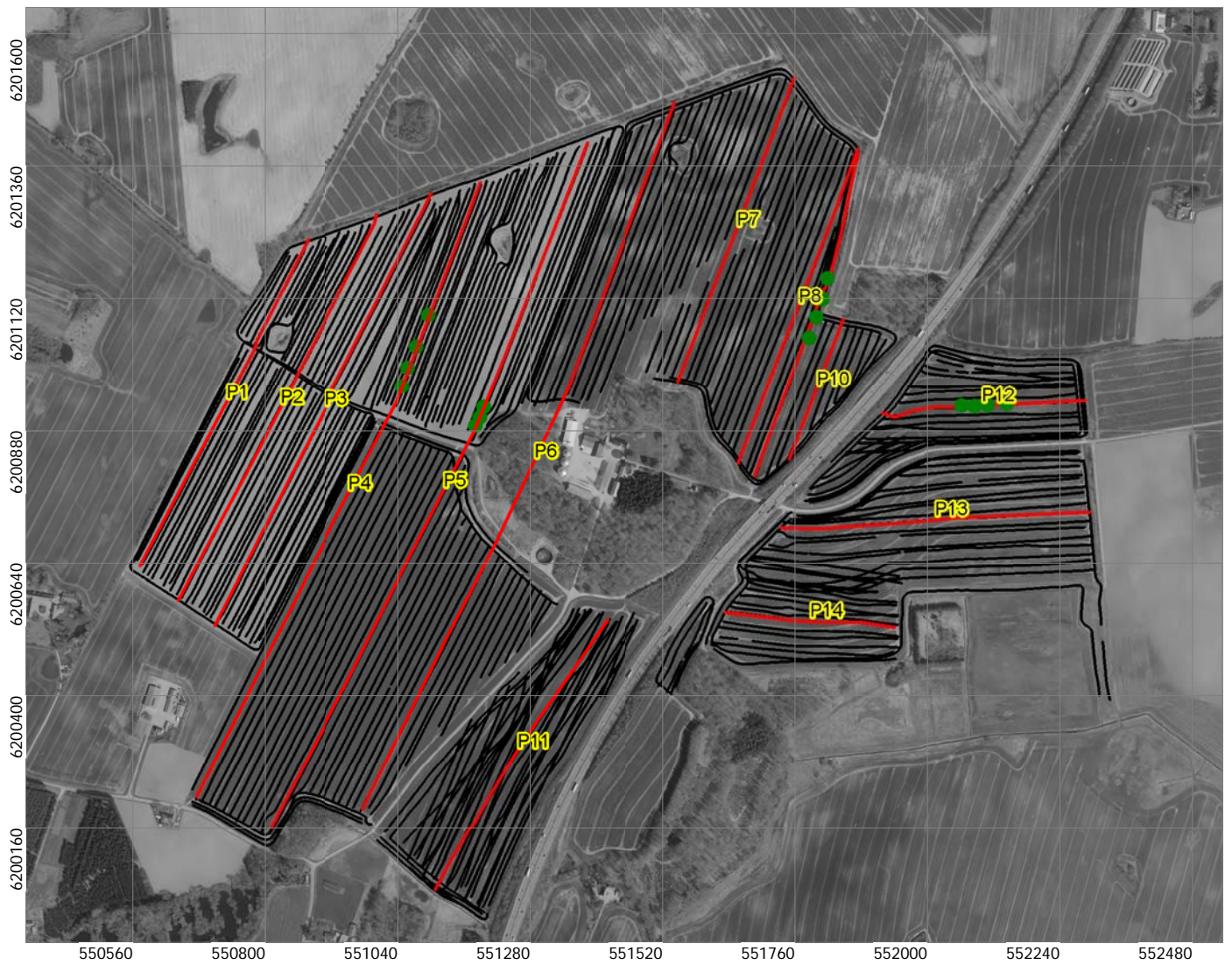


GCM Gedved 2017

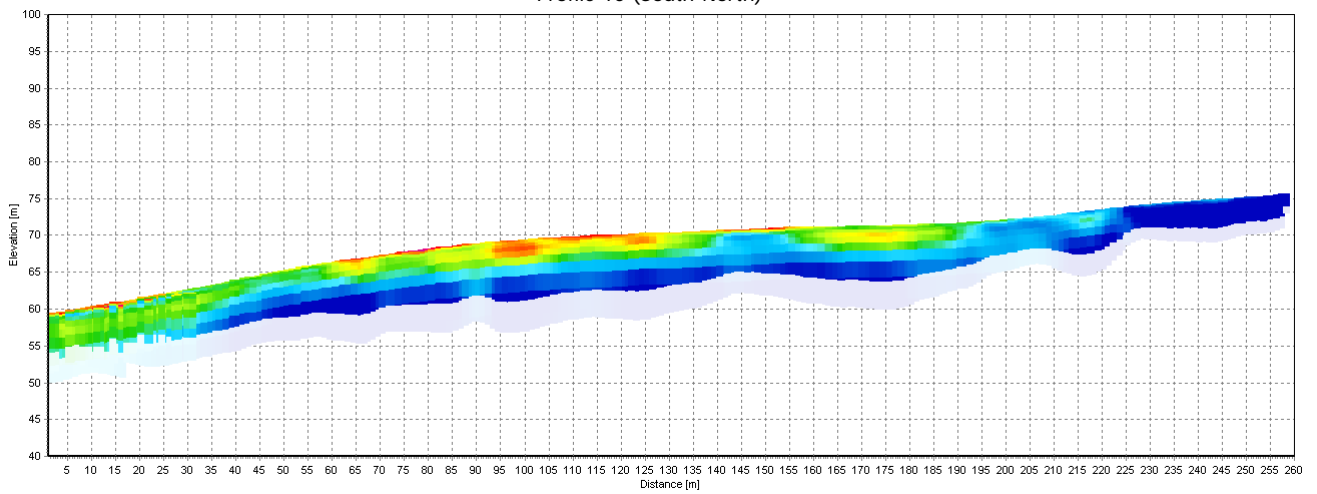


Resistivity Profiles (ohmm)
Smooth SCI Model

The profiles display model bars from the smooth inversion results
Models have been blanked by 75% below the DOI Standard
Borehole information - Blue:Clay Brown:Plowlayer Red:Sand



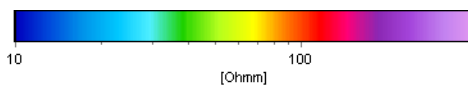
Profile 10 (South-North)



HydroGeophysics Group
AARHUS UNIVERSITY

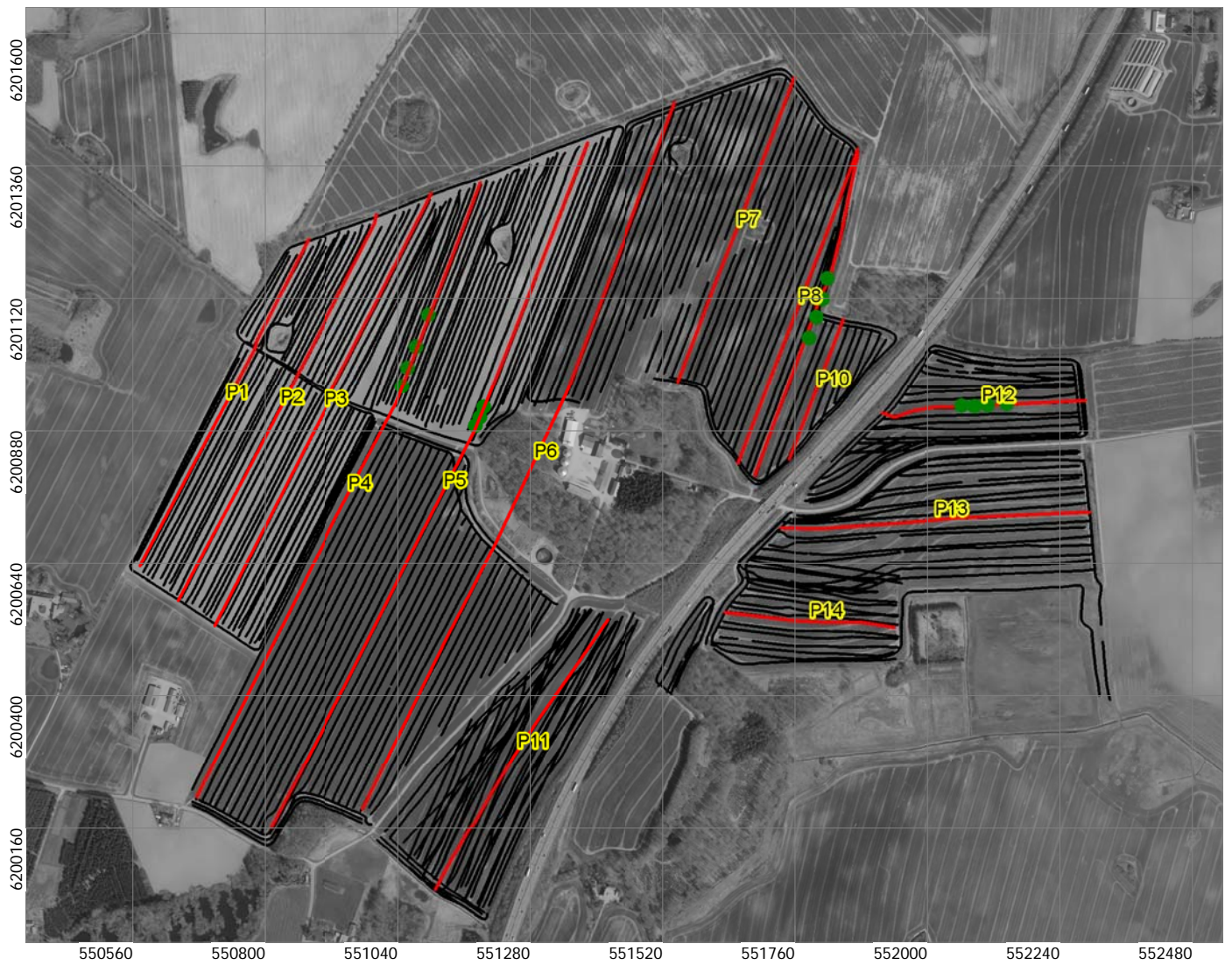


GCM Gedved 2017

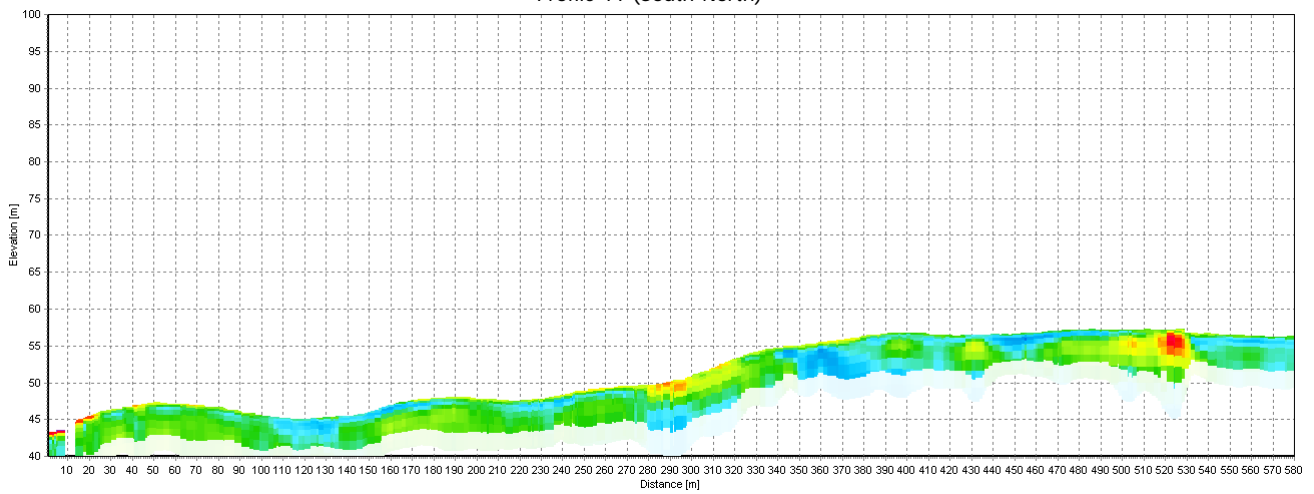


Resistivity Profiles (ohmm)
Smooth SCI Model

The profiles display model bars from the smooth inversion results
Models have been blanked by 75% below the DOI Standard



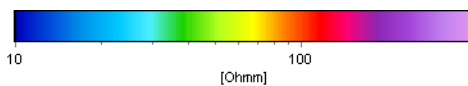
Profile 11 (South-North)



HydroGeophysics Group
AARHUS UNIVERSITY

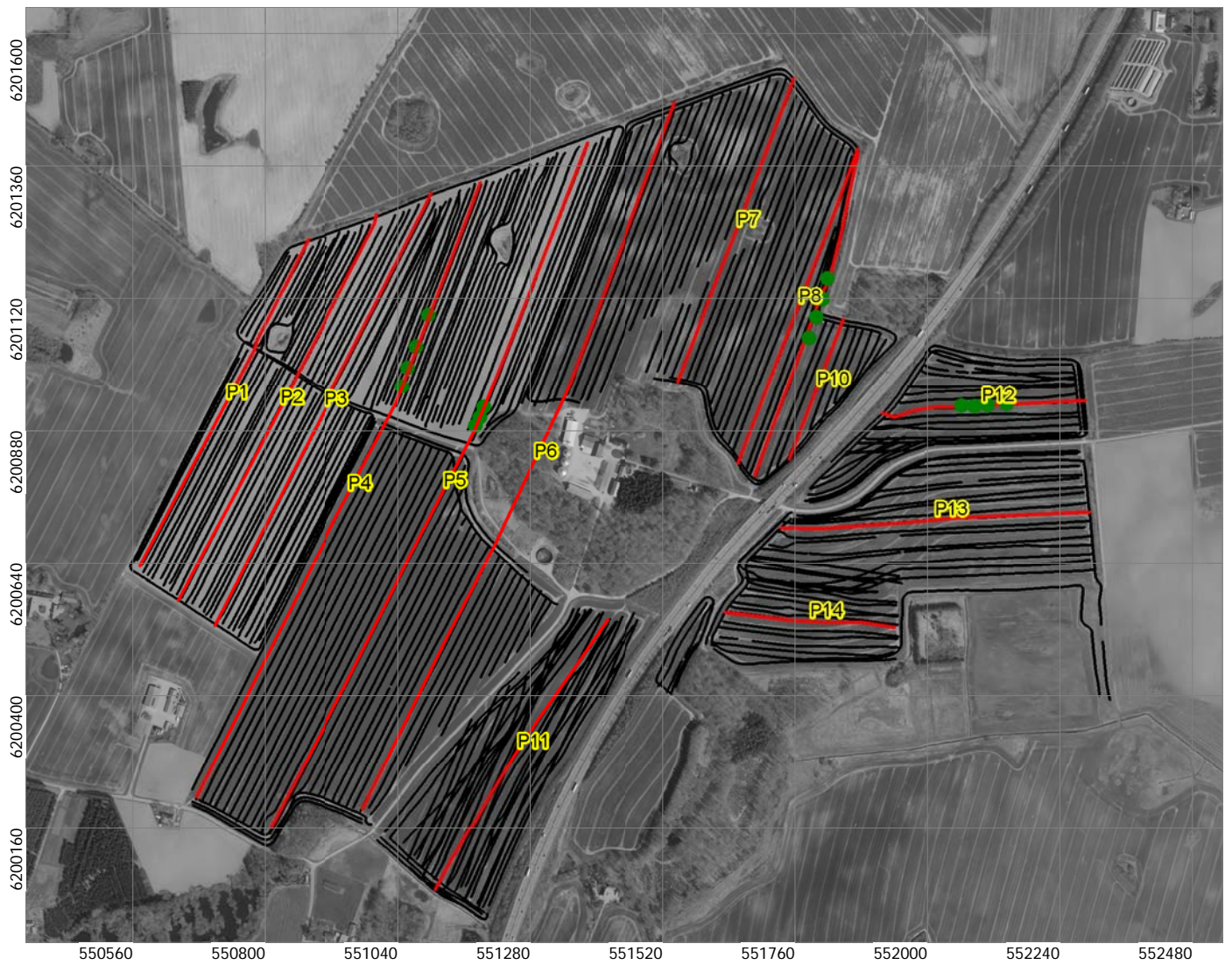


GCM Gedved 2017

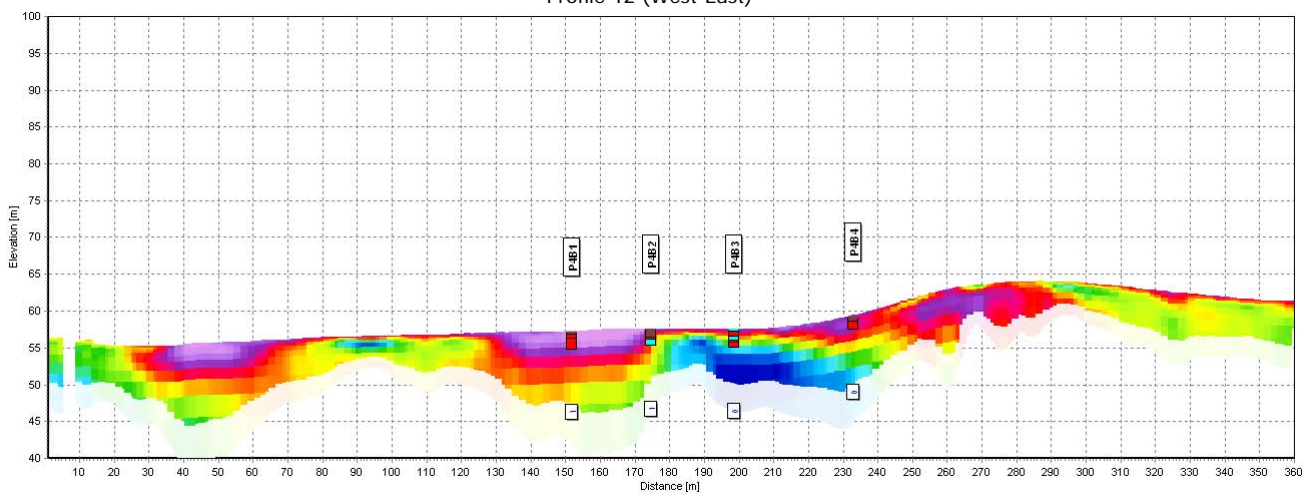


Resistivity Profiles (ohmm)
Smooth SCI Model

The profiles display model bars from the smooth inversion results
Models have been blanked by 75% below the DOI Standard



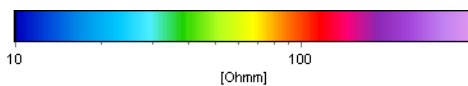
Profile 12 (West-East)



HydroGeophysics Group
AARHUS UNIVERSITY



GCM Gedved 2017



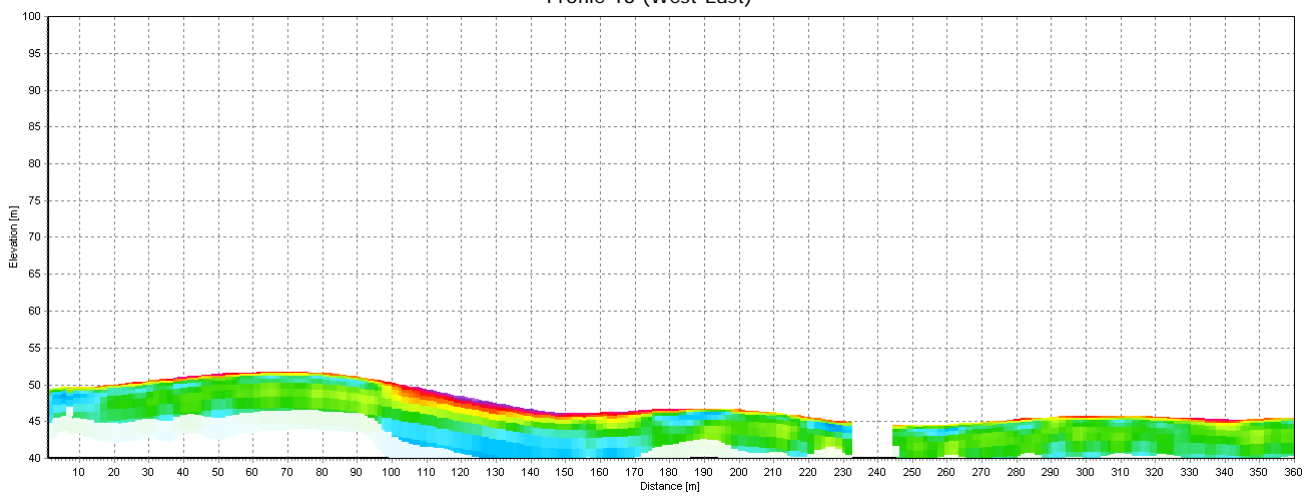
Resistivity Profiles (ohmm)

Smooth SCI Model

The profiles display model bars from the smooth inversion results
Models have been blanked by 75% below the DOI Standard
Borehole information - Blue:Clay Brown:Plowlayer Red:Sand



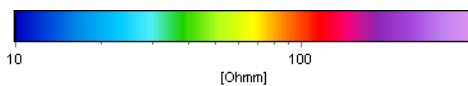
Profile 13 (West-East)



HydroGeophysics Group
AARHUS UNIVERSITY



GCM Gedved 2017

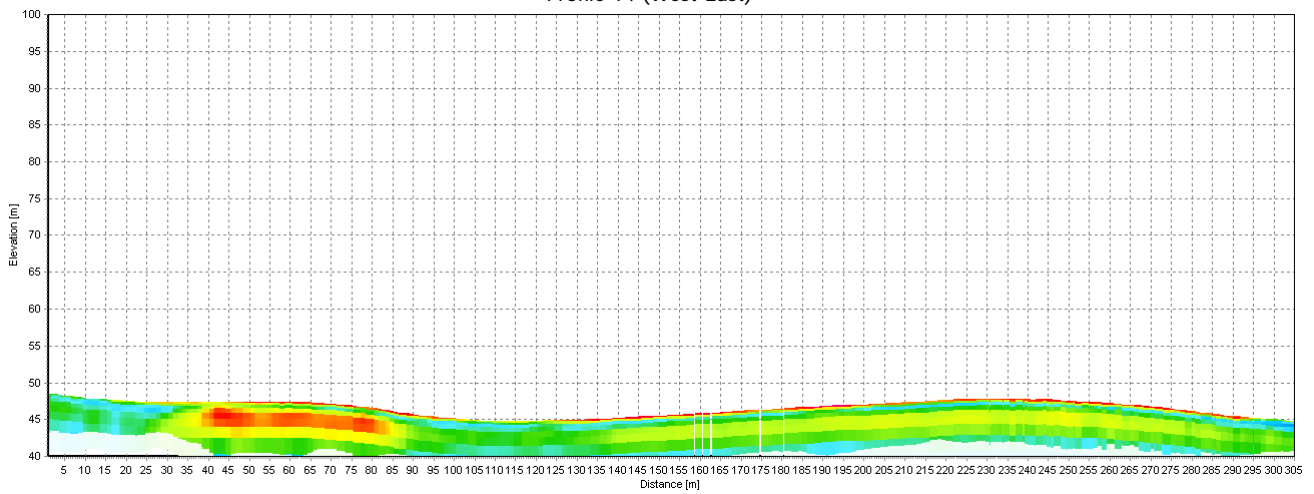


Resistivity Profiles (ohmm)
Smooth SCI Model

The profiles display model bars from the smooth inversion results
Models have been blanked by 75% below the DOI Standard



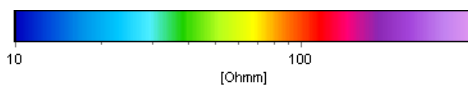
Profile 14 (West-East)



HydroGeophysics Group
AARHUS UNIVERSITY



GCM Gedved 2017



Resistivity Profiles (ohmm)
Smooth SCI Model

The profiles display model bars from the smooth inversion results
Models have been blanked by 75% below the DOI Standard